Monocyte-derived peritoneal macrophages protect C57BL/6 mice against surgery-induced adhesions

Rinal Sahputra[1,2*], Krittee Dejyong[1,3], Adrian S Woolf[1,4], Matthias Mack[5], Judi Allen[2], Dominik Ruckerl[2*], Sarah E Herrick[1,2*]

[1]Division of Cell Matrix Biology and Regenerative Medicine, School of Biological Sciences and Manchester Academic Health Science Centre, Faculty of Biology, Medicine and Health, The University of Manchester, Manchester, UK

[2]Lydia Becker Institute of Immunology and Inflammation, School of Biological Sciences, and Manchester Academic Health Sciences Centre, Faculty of Biology, Medicine and Health, The University of Manchester, Manchester. UK

[3] Faculty of Veterinary Science, Prince of Songkla University, Songkhla, Thailand

[4]Royal Manchester Children's Hospital, Manchester University NHS Foundation Trust, Manchester. UK

[5]Department of Nephrology, Universitätsklinikum Regensburg, Regensburg, Germany

[*]Corresponding authors:

Rinal Sahputra, rinal.sahputra@manchester.ac.uk, Stopford Building- 3.107, The University of Manchester. Oxford Road, Manchester. Tel : 0161 275 1593

Dominik Ruckerl, dominik.ruckerl@manchester.ac.uk, AV Hill Building-4.013, The University of Manchester. Oxford Road, Manchester. Tel : 0161 276 0098

Sarah E Herrick, sarah.herrick@manchester.ac.uk, Stopford Building- 3.106, The University of Manchester. Oxford Road, Manchester. Tel : 0161 275 1528

Short running title: Monocyte-derived macrophages prevent peritoneal adhesion formation

Conflict of Interest statement: There is no commercial or financial conflict of interest.

Abstract

Peritoneal adhesions commonly occur after abdominal or pelvic surgery. These scars join internal organs to each other or to the cavity wall and can present with abdominal or pelvic pain, and bowel obstruction or female infertility. The mechanisms underlying adhesion formation remain unclear and thus effective treatments are not forthcoming. Peritoneal macrophages accumulate after surgery and previous studies have attributed either pro- or anti-scarring properties to these cells. We propose that there are complex and nuanced responses after surgery with respect to both resident and monocyte-derived peritoneal macrophage subpopulations. Moreover, we contend that differences in responses of specific macrophage populations, in part, explain the risk of developing peritoneal scars. We characterised alterations in peritoneal macrophage subpopulations after surgery-induced injury using two strains of mice, BALB/c and C57BL/6, with known differences in macrophage response post-infection. At 14 days post-surgery, BALB/c mice displayed more adhesions compared with C57BL/6 mice. This increase in scarring correlated with a lower influx of monocyte-derived macrophages at day 3 post-surgery. Moreover, BALB/c mice showed distinct macrophage repopulation dynamics after surgery. To confirm a role for monocyte-derived macrophages, we used *Ccr2*-deficient mice as well as antibody-mediated depletion of CCR2 expressing cells during initial stages of adhesion formation. Both *Ccr2*-deficient and CCR2-depleted mice showed a significant increase in adhesion formation associated with the loss of a peritoneal monocyte influx. These findings reveal an important protective role for monocyte-derived cells in reducing adhesion formation after surgery.

Keywords: peritoneum, macrophages, adhesion formation, monocytes, surgery, post-operative, mouse

Introduction

Peritoneal adhesions commonly occur after abdominal or pelvic surgery and abnormally conjoin internal organs to each other or to the adjacent cavity wall. Adhesions may cause a range of complications, including severe chronic pelvic pain, female infertility, intestinal obstruction, and are a contraindication for future abdominal surgery [1]. The peritoneum lines the cavity wall and majority of internal organs, and consists of a surface monolayer of mesothelial cells overlaying a layer of submesothelial connective tissue [2]. During surgery, this gliding interface is disrupted and adhesions may develop from fibrin-rich clots that span between injured tissues [3]. Several key events, including reduced fibrinolysis [4] and mesothelial-to-mesenchymal transition (MMT) [5, 6], have been shown to be pivotal in adhesion formation. However, cellular and molecular pathways underlying their development are not well defined. Consequently, attempts to prevent adhesions occurring, such as atraumatic surgical technique and use of barrier material, show mixed success and hence are not consistently applied [1]. An improved understanding of surgical adhesion formation will lead to better prevention strategies.

Peritoneal macrophages, although known to provide immune surveillance of the abdominal cavity [7], are also involved in the formation of post-surgical adhesions [8-10]. Critically, however, there is a lack of consensus as to their exact contribution, with studies attributing both protective as well as pathological roles to macrophages. Experimental expansion of peritoneal macrophages has been shown to have protective effects [9, 11], while somewhat in contradiction, depletion of peritoneal macrophages also reduces adhesion formation [12]. The peritoneal cavity contains at least three macrophage subpopulations: a long-lived, self-renewing resident population (F4/80^{high}) also known as large peritoneal macrophages, a population derived from monocytes recruited from the blood (F4/80^{low}), also known as small peritoneal macrophages [13], and an intermediate population (F4/80^{int}), which consists of monocyte-derived macrophages in the process of differentiating into a cavity resident phenotype [14]. Functional differences between these subsets [14-16] and time of analysis may explain the contradictory outcome of studies that have manipulated macrophage

numbers. However, which specific subsets are responsible for protective or pathologic properties remains unclear. Notably, fundamental differences exist between common laboratory mouse strains, BALB/c and C57BL/6, in terms of the response of serous cavity macrophages to infection [17, 18]. Here, we investigated the dynamics of peritoneal macrophage subsets in BALB/c and C57BL/6 mice after performing surgery to induce adhesions. To confirm a role for monocyte-derived macrophages, we analysed surgical adhesion formation in *Ccr2*-deficient mice as well as in monocyte-depleted C57BL/6 mice.

Materials and Methods

Experimental animals

Female BALB/c and C57BL/6 mice, 10 to 12 weeks of age, were purchased from Envigo, Hillcrest, UK. The *Ccr2*-knock out *(*KO) colony (originally from The Jackson Laboratory, USA and provided by J. Grainger, The University of Manchester, UK) was backcrossed to a C57BL/6 background for at least 10 generations and maintained in-house using breeding pairs of heterozygous mice. Ten-to twelve-week-old KO mice and their wild-type (WT) littermates were used. All animals were maintained in individually ventilated cages under specific-pathogen-free conditions in the Biological Services Facilities of the University of Manchester and provided with food and water *ad libitum*. Animal experiments were performed according to the UK Animals (Scientific Procedures) Act (1986) under a Project License (P1208AD89) granted by the UK Home Office and approved by the University of Manchester Ethical Review Committee.

Surgical procedure

Abdominal surgery was performed following a previously described protocol with slight modification [19, 20]. Briefly, under anaesthesia, a midline incision was created followed by circular wounding approximately 7 mm^2 of the left peritoneal cavity wall (approximately 1 cm caudal to the xiphoid cartilage and 1 cm from the incisional line) using a trauma instrument developed in-house.

Thereafter, approximately 1 cm length of caecum serosa was abraded with a No 15 surgical blade and then surgically attached to the wounded peritoneum wall using two sutures horizontally placed 3-5 mm each side of the peritoneal wound through the abdominal and caecal submucosa. Linea alba and skin were closed separately. The mice were necropsied at day 3, day 7, and day 14 post-surgery.

Antibody depletion of monocytes

To assess the importance of monocyte-derived peritoneal macrophages during surgery-induced adhesion formation, female C57BL/6 mice were treated with 20 μg of α-CCR2 mAb (clone: MC21, RRID:AB_2314128; [21] or isotype control antibody (Rat IgG2b, Biolegend) in 200 μl of PBS via daily intra-peritoneal (i.p.) injection at day -1, 0, and day 1 post-surgery.

Peritoneal lavage and adhesion score measurement

Collection of peritoneal lavage fluid and peritoneal exudate cells (PECs) was performed by flushing the peritoneal cavity 3 times. The first 3 ml of the wash was centrifuged, and supernatant used for the detection of soluble mediators using ELISA. The remaining cell pellet was collected by centrifugation for flow cytometry analysis. After erythrocytes removal, cell number was determined using a Countess II FL automated cell counter (Invitrogen). Adhesion score was assessed by two independent observers according to the scoring scheme depicted in supplementary Table 1. Adhesion tissue was collected and fixed in 4% buffered paraformaldehyde before being processed and embedded in paraffin wax for histology analysis.

Flow cytometry

An aliquot ($1x10^6$) of total PECs were stained using a viability assay (Zombie UV, Biolegend) and blocked with 5 μg/mL anti-CD16/32 (clone 93; Biolegend) and heat inactivated normal mouse serum (1:10, Sigma-Aldrich) in flow cytometry buffer before surface staining on ice with antibodies listed in supplementary Table 2 and 3. For intracellular staining, samples were fixed and

permeabilised using eBioscience Foxp3 Staining Buffer kit (Fisher Scientific) before adding antibodies in 1x eBioscience™ Permeabilization Buffer (Thermo Fisher Scientific). All antibodies were purchased from Biolegend unless stated otherwise. PECs were analysed on a BD FACSymphony machine using BD FACSDiva software (BD Biosciences) and post-acquisition analysis performed using FlowJo v10 software (BD Biosciences). The gating strategy for flow cytometry analysis is shown in supplementary Figure 1.

Histological analysis

Serial sections (5-µm-thick) of peritoneal adhesion tissue were collected, de-waxed and rehydrated using serial dilutions of alcohol prior to Masson's trichrome staining following manufacturer's instruction (Sigma-Aldrich). Images were acquired using a [20×/0.80 Plan Apo] objective using the Pannoramic 250 Flash II slide scanner (3D Histech Ltd., Hungary). Collagen profile was analysed by quantifying the selected adhesion area in μm^2 using RGB thresholding by QuantCentre and HistoQuant plugin on SlideViewer software (version 2.5).

Detection of soluble mediators

Interleukin (IL)-6, IL-10, IL-12, IL-13, TNF-α, IFN-γ, Relmα and Ym1 in peritoneal lavage fluid were detected by enzyme linked immunosorbant assay (ELISA) in ninety-six-well immunoGrade plates (BrandTech Scientific, Inc). List of coating and detection antibodies is shown in supplementary Table 4. After adding stop solution, plates were read at 450 nm on a VersaMax Microplate reader (Molecular Devices).

Statistical analysis

Statistical analysis was performed using Prism 9 (Graph-Pad software Inc., La Jolla, CA). Normal distribution of residuals was assessed by Shapiro-Wilk test. Significant differences between two groups ($p<0.05$) were analysed using t-test or ANOVA followed by Tukey posthoc test for

experiments with more than 2 groups. Data with non-Gaussian distribution were analysed using Mann Whitney test or Kruskal-Wallis ANOVA followed by Dunn's multiple comparison test. Differences with a p-value of less than 0.05 were considered statistically significant.

Results

Early monocyte influx in C57BL/6 mice is associated with fewer peritoneal adhesions

To determine whether BALB/c and C57BL/6 mice showed differences in susceptibility to peritoneal adhesions, and if this related to variations in macrophage subset responses, mice of each strain were subjected to surgical injury. Three, 7 and 14 days after surgery, animals were analysed for adhesion formation between injured sites on the caecum and peritoneal cavity wall (site-specific) as well as to other organs or midline incision (non-site-specific) (see scoring system, supplementary Table 1). Similar to previously published data [22], we found that BALB/c mice were more likely to develop peritoneal adhesions compared with C57BL/6 mice. However, in our model this enhanced susceptibility did not become apparent until day 14 after surgery (Figure 1A). Collagen profile in site-specific adhesion tissue, as assessed by Masson's trichrome staining, was similar between the two strains at day 3 and 7 post-surgery (supplementary Figure 2). However, BALB/c mice showed significantly higher collagen deposition in site-specific adhesion tissue at day 14 (Figure 1B, C).

Although there was no significant difference in the total number of PECs between BALB/c and C57BL/6 prior to and after surgery (supplementary Figure 3), BALB/c mice showed a significantly lower number of total peritoneal macrophages (CD11b+Lin-Ly6C-) under steady state conditions as well as on day 3 post-surgery (Figure 1D). This difference was largely due to reduced numbers of cavity resident macrophages (F4/80^{high}), however these reached similar numbers in both strains from day 7 (Figure 1E). Moreover, although both strains of mice showed recruitment of monocytes (CD11b+Lin-MHCII-F4/80-Ly6C^{high}) from day 3 with the number staying elevated up to day 14, the early influx of monocytes (day 3) was significantly more pronounced in C57BL/6 compared with BALB/c mice (Figure 1F). Infiltrating monocytes have been shown to differentiate

into mature macrophages (F4/80^{low}) within the cavity [23] and recruited monocytes can also give rise to resident macrophages (F4/80^{high}) via an intermediate population (F4/80^{int}) [14]. In line with the enhanced early influx of monocytes, C57BL/6 mice also showed an enhanced total cell number of F4/80^{low} (Figure 1G) and F4/80^{int} macrophages (Figure 1H) at day 3.

C57BL/6 mice show altered macrophage phenotypes in line with enhanced monocyte-to-F4/80^{high} macrophage conversion

Changes in macrophage dynamics, in particular the loss of F4/80^{high} cavity resident macrophages after surgery, has previously been reported with C57BL/6 mice [24]. However, specific differences between BALB/c and C57BL/6 mice have not been investigated; hence we performed a more in-depth characterisation of dynamic changes in peritoneal macrophage subsets following surgery in the two strains. CD102, and the transcription factor Gata6, are known as defining markers of F4/80^{high} cavity resident macrophages, upregulated at different stages of the differentiation process [25]. Both markers were expressed at similar levels by F4/80^{high} macrophages present in both BALB/c and C57BL/6 mice (Figure 2A, B), indicating that although surgery induced considerable changes in the number of these cells with reduced numbers in BALB/c at day 3 (Figure 1E), they retained their peritoneal cavity resident identity. However, at day 3 after surgery F4/80^{high} macrophages of both strains showed a dramatic loss in the proportion of cells expressing Tim4, another defining marker of F4/80^{high} cavity resident macrophages (Figure 2C). Of note, F4/80^{high} macrophages in BALB/c mice regained Tim4 expression over the course of the study with expression at day 14 similar to naïve mice (Figure 2C). In contrast, this recovery of Tim4+ F4/80^{high} cells did not occur in C57BL/6 mice (Figure 2C). Expression of Tim4 by F4/80^{high} macrophages has been implicated as a marker of an embryonic origin and established resident peritoneal population, whereas monocyte-derived resident macrophages largely fail to express Tim4 [14]. Thus, persistent loss of Tim4 expression in F4/80^{high} cavity macrophages of C57BL/6 mice might indicate an enhanced integration of monocyte-derived cells into the resident macrophage pool.

CD226 (aka DNAM-1) is highly expressed by F4/80^{low} macrophages present in the peritoneal cavity under steady state conditions [26] and CD226+ cells are known to undergo the macrophage disappearance reaction under inflammatory conditions [27]. In line with this, the proportion of CD226+ F4/80^{low} macrophages was reduced at day 3 after surgery, and there was no significant difference between C57BL/6 and BALB/c mice (Figure 2D) suggesting that both mouse strains show the macrophage disappearance reaction to a similar degree. Semaphorin 4a (Sema4a), is expressed by circulating inflammatory monocytes and is upregulated on peritoneal macrophages during inflammation [28]. Furthermore, it is retained during resolution of inflammation on F4/80^{int} and F4/80^{high} cells of monocytic origin [14]. In line with a lower monocyte-derived macrophage influx on day 3, BALB/c mice showed fewer Sema4a+F4/80^{low} macrophages, whereas Sema4a expression was maintained on F4/80^{low} macrophages in C57BL/6 mice (Figure 2E). Similarly, Lymphatic Vessel Endothelial Receptor 1 (Lyve-1) expression has been associated with differentiation of monocyte-derived cells to F4/80^{int} macrophages [18]. Interestingly, we found a significant decrease in Lyve-1 expression by F4/80^{low} macrophages in C57BL/6 mice compared with BALB/c mice on day 14 (Figure 2F) but found no difference in the proportion of F4/80^{int} or F4/80^{high} macrophages expressing Lyve-1 between the strains (supplementary Figure 4). Of note, we found that none of the markers previously associated with specific macrophage subsets (e.g. CD102, Tim4, Lyve-1) were exclusively expressed by only one peritoneal macrophage subset (F4/80^{low}, F4/80^{int}, F4/80^{high}) but were shared between several subsets (supplementary. Figure 5). This indicates a certain degree of phenotypic plasticity between the described macrophage subsets rather than exclusive expression patterns.

Regarding cellular activation, we did not detect a significant induction of either M1 (Sca1, TNFα) or M2 (Relmα, Ym1, CD206) activation markers in response to surgery in either BALB/c or C57BL/6 mice (Figure 2 G-I, supplementary. Figure 4). However, BALB/c mice showed a significantly lower number of Sca-1+ myeloid cells (CD11b+lin-Ly6C- cells) prior and at day 3 (Figure 2G), as well as a lower number of Relmα+ cells at day 3 (Figure 2H) and lower numbers of Ym1+ cells at day 14 after surgery compared with C57BL/6 (Figure 2I). We also analysed cytokine

levels in peritoneal lavage of BALB/c and C57BL/6 mice prior and after surgery (Figure 2J, K, supplementary Figure 6). Interestingly, the level of Relmα in the peritoneal lavage of BALB/c mice was significantly lower compared with C57BL/6 at day 7 post-surgery (Figure 2J), a slight delay compared with the Relmα+ cell reduction found at day 3 with flow cytometry (Figure 2H). Similar to the flow cytometry data (Figure 2I), a significantly lower concentration of Ym-1 in peritoneal lavage of BALB/c mice was detectable at day 14 compared with C57BL/6 (Figure 2K). The remaining cytokines did not show a significant difference in levels between BALB/c and C57BL/6 mice prior and post-surgery (supplementary. Figure 6).

Genetically altered mice lacking circulating monocytes develop significantly more adhesions

Our findings indicated that BALB/c mice were more likely to have increased peritoneal adhesions at day 14 after surgery, compared with C57BL/6 mice, potentially due to reduced monocyte infiltration early following surgery. Therefore, adhesion-inducing surgery was performed in *Ccr2*-deficient mice (*Ccr2*KO on a C57BL/6 background). Due to the targeted disruption of the CCR2 gene, *Ccr2*KO mice fail to recruit monocytes to sites of inflammation/injury, in part because of defective egress from the bone marrow [29]. As expected, following surgery, *Ccr2*KO mice showed a significantly higher peritoneal adhesion score at day 7 compared with WT littermates (Figure 3A, B). *Ccr2*KO mice also showed a significantly higher relative percentage of F4/80^{high} macrophages after surgery (Figure 3C), but there was no significant difference in total number of F4/80^{high} resident macrophages between *Ccr2*KO and WT littermates prior and post-surgery (Figure 3G). Thus, it seems unlikely that the difference in adhesion formation was due to changes in the dynamics of F4/80^{high} resident macrophages. In contrast, and in line with reduced monocyte infiltration, the relative percentage and total number of infiltrating monocytes (Figure 3D, H), F4/80^{low} monocyte-derived macrophages (Figure 3E, I), and F4/80^{int} converting cells (Figure 3F, J) were significantly lower in *Ccr2*KO compared with WT littermates after surgery. Data thus supports the hypothesis that

infiltrating monocyte-derived cells play a protective role in surgery-induced peritoneal adhesion formation.

Monocyte-to-F4/80^{high} macrophage conversion was abrogated in *Ccr2*KO mice

As expected, the lack of *Ccr2* expression in *Ccr2*KO mice reduced monocyte influx into the peritoneal cavity compared with WT littermates. Consequently, similar to our data with BALB/c mice (Figure 2C), the relative percentage of Tim4+ cells within F4/80^{high} macrophages at day 7 after surgery in *Ccr2*KO mice was significantly higher compared with WT littermates (Figure 4A). The lack of monocyte influx in *Ccr2*KO mice also caused a significantly lower relative percentage of Sema4a+ cells within F4/80^{low} (Figure 4B), F4/80^{int} (Figure 4C), and F4/80^{high} (Figure 4D) macrophage subsets compared with WT littermates. In addition, the relative percentage of Lyve-1+ cells within F4/80^{low} (Figure 4E), F4/80^{int} (Figure 4F), and F4/80^{high} (Figure 4G) macrophage subsets in *Ccr2*KO mice was also significantly lower compared with WT littermates. The relative percentage of CD226+ cells within F4/80^{low} macrophage population did not show any significant difference between groups (Figure 4H), but *Ccr2*KO mice had significantly lower total number of CD226+ cells compared with WT littermates (Figure 4I). We also analysed the activation of all macrophage populations and found that *Ccr2*KO peritoneal macrophages had significantly lower CD206 (Figure 4J) and Relmα expression (Figure 4K) prior and post-surgery compared with WT littermates. Similar to our flow cytometry data, the level of Relmα in the peritoneal lavage were also significantly lower in *Ccr2*KO at day 7 compared with WT littermates (Figure 4L). The levels of the other cytokines, including Ym1, IFN-γ, IL-6, IL-10, IL-12, and IL-13 remained the same between the groups (supplementary. Figure 7).

Depletion of monocyte-derived peritoneal macrophages induced more peritoneal adhesions post-surgery

As *Ccr2*KO mice do not express the *Ccr2* gene, monocyte influx is defective throughout their life course thus, it is not possible to determine whether early influx of monocytes, as observed in C57BL/6 mice on day 3 post-surgery (Figure 1F), was contributing to the reduction in adhesions or whether influx of monocytes at a later stage (day 7 or 14 post-surgery) was also of importance. In addition, due to effects on their replenishment, phenotypically distinct resident macrophages accumulate in *Ccr2*KO animals with age [25]. Therefore, the observed susceptibility to adhesion formation may have been due to altered functional responses of cavity resident macrophages in *Ccr2*KO mice rather than defective monocyte recruitment. To address this issue, C57BL/6 mice were treated with an anti-CCR2 monoclonal antibody (mAb; clone MC21; [21]) injected i.p. at day -1, 0, and 1 after surgery to specifically deplete monocytes during the early phases of repair. Rat IgG2b was used as isotype control, and mice were analysed at day 14 (Figure 5A). MC21 mAb has been shown to effectively deplete CCR2+ (CD11b+Ly6C^{high}) monocytes [21]. Similar to our findings with BALB/c and *Ccr2*KO mice, early depletion of infiltrating monocytes enhanced susceptibility of C57BL/6 mice to surgery-induced adhesions at day 14 compared with isotype control antibody treated mice (Figure 5B, C). Moreover, site-specific adhesion tissue in anti-CCR2 mAb treated mice also showed significantly higher collagen deposition at day 14 compared with isotype control treated mice (Figure 5C, D). Both at day 3 as well as day 14, no significant difference in total number of PECs (Figure 5E), F4/80^{high} macrophages (Figure 5F) or monocytes (Figure 5G) could be detected between groups. However, anti-CCR2 mAb treated mice regained significantly higher Tim4 expression within the F4/80^{high} macrophage subset at 14 days compared with isotype control treated mice (Figure 5H), indicative of reduced monocyte integration in anti-CCR2 Ab treated mice. Of note, unlike BALB/c (Figure 2C) and *Ccr2*KO mice (Figure 4A), anti-CCR2 mAb treated mice only partially regained Tim4 expression (~ 44%) and did not reach the same level as detected in naïve C57BL/6 mice (~ 92%, Figure 2C), suggesting a delayed integration of monocyte-derived cells. In line with this hypothesis, no significant difference in any of the other peritoneal macrophage markers (e.g. Sema4a, Lyve-1) was found between anti-CCR2 mAb treated and isotype control-treated mice after surgery

(supplementary Figure 8 and 9). Interestingly, the level of Relmα in the peritoneal lavage of anti-CCR2 mAb-treated mice at day 14 was significantly higher compared with isotype control-treated mice (Figure 5I), which may indicate a delay in the induction of surgery-induced responses (Figure 2J) or over-compensatory mechanisms. All other cytokines remained similar between the groups (supplementary. Figure 10). Together, the treatment of C57BL/6 mice with a monocyte-depleting antibody thus provided direct evidence that monocytes contribute to protection against adhesion formation.

Discussion

The contribution of peritoneal macrophages to adhesion formation after surgery remains ill-defined, with both a protective and pathological role reported [9, 11, 12]. Furthermore, mouse strain differences in susceptibility to surgical adhesion formation was previously demonstrated [22], but the mechanisms driving these differences remain largely unexplored. Here, we found that C57BL/6 mice showed a significantly lower peritoneal adhesion score at day 14 after surgery compared with BALB/c mice. Moreover, site-specific adhesions that did form displayed a relatively lower collagen deposition suggesting the adhesions maybe less mature and more readily degraded. Importantly, C57BL/6 mice showed an enhanced influx of monocytes and monocyte-derived macrophages at day 3. Blocking the recruitment of circulating monocytes in C57BL/6 mice, either by using *Ccr2*KO mice or antibody-mediated CCR2 depletion, resulted in an enhanced susceptibility to peritoneal adhesions after surgery. Together, these data provide evidence that circulating monocytes or monocyte-derived macrophages help prevent peritoneal adhesions following surgery (Figure 6).

Our data complements and advances two previous studies of surgery-induced adhesion formation, in which experimental enhancement of monocyte recruitment showed a protective effective. In a rabbit study, recruitment of inflammatory cells, including monocytes, by intraperitoneal injection of protease peptone prior to surgery reduced the number of peritoneal adhesions formed [9]. In a mouse model of ischaemic button- induced adhesion formation,

thioglycolate or monocyte chemoattractant protein-1 (MCP-1) injection increased inflammatory monocyte influx and reduced adhesion formation [11]. In this latter study, transient neutrophil depletion was also proposed as a complementary mechanism for reducing adhesions [11]. In this context, it is interesting to note, that although BALB/c mice were more susceptible to peritoneal adhesions in our model, an equivalent increase in neutrophils in the peritoneal cavity at day 3 after surgery was found compared with C57BL/6 mice (supplementary. Figure 11). Moreover, *Ccr2*KO mice have been shown to recruit equivalent numbers of neutrophils in a model of bacteria-induced inflammation [30]. Thus, the protective effect of monocytes or monocyte-derived cells in our model seems unlikely to be dependent on an altered neutrophil response.

Similarly, two recent studies suggested that rapid recruitment of F4/80^{high} peritoneal resident macrophages to the site of mesothelial injury may result in the creation of a barrier preventing excessive fibrin attachment and consequently preventing the formation of adhesions after surgery [24, 31]. We found that C57BL/6 mice showed a significantly higher number of peritoneal F4/80^{high} resident macrophages prior and at day 3 post-surgery compared with BALB/c mice. Thus, C57BL/6 mice may be inherently protected from peritoneal adhesion formation by forming a macrophage-rich barrier. However, the number and dynamics of the resident macrophage population in both *Ccr2*KO and antibody-depleted mice were not altered compared with their respective controls, while these mice were still more susceptible to adhesion formation. Our data from *Ccr2*KO and anti-CCR2 mAb depleted animals, both on a C57BL/6 background, therefore argue for an additional protective role for monocytes and monocyte-derived cells as described, independent of a possible protective barrier function of F4/80^{high} resident macrophages.

Of note, we found that the difference in adhesion score between BALB/c and C57BL/6 mice occurred at a later stage of adhesion formation (day 14 post-surgery). Whilst the adhesion score in BALB/c mice remained the same between day 7 and day 14 after surgery, C57BL/6 mice showed a reduced adhesion score at day 14 suggesting that some adhesions that initially formed in C57BL/6 may have been immature and cleared possibly due to lower collagen deposition that stabilises

development. Clearance of early fibrin-rich adhesions has been associated with increased fibrinolysis in the initial stages post-surgery [4] and so the protective effect of monocytes or monocyte-derived macrophages may be due to promotion of proteolytic activity and hence degradation of collagen-poor unstable adhesions between days 7 and 14 post-surgery. This proposal is consistent with the finding that monocyte-derived macrophages degrade fibrin-rich aggregates that form in response to intraperitoneal bacterial infection [32]. Interestingly, the response of resident F4/80^{high} Gata6-dependent macrophages was found to depend on the severity of the insult [31]. Thus, the protective effects of monocytes or monocyte-derived macrophages in our model may be explained by active degradation of immature adhesions through proteolytic activity or by disrupting F4/80^{high} resident macrophage-derived superaggregates.

Importantly, we cannot distinguish whether the protective effect is mediated via monocytes themselves or via macrophages that have differentiated from monocytes in the cavity. Furthermore, differences in the recruitment of monocytes to the peritoneal cavity between BALB/c and C57BL/6 mice were largely restricted to the early phases of the repair process (day 3 post-surgery, Figure 1F) and early but transient depletion of monocytes significantly affected adhesion formation (Figure 5B). Changes in monocyte-derived macrophage populations (F4/80^{low} and F4/80^{int}) were slightly prolonged, but similarly temporary (Figure 1G, H). Thus, it is unclear if these cells act early during the adhesion formation process, but the outcome of these actions was not visible until later (day 14 post-surgery), or whether the cells acquire an activation phenotype at later stages dependent on their earlier influx. Interestingly, we found a marked change in the phenotype of F4/80^{high} resident macrophages at later stages, as indicated by the loss of Tim4 expression by these cells (Figure 2C). Tim4 has been linked to the embryonic origin of resident macrophages, while a loss of Tim4 expression indicates integration of monocyte-derived macrophages into the resident pool [23]. Thus, the maintained expression of Tim4 by F4/80^{high} macrophages in BALB/c, *Ccr2*KO, and partially in anti-CCR2 mAb-treated mice indicates a failure to integrate monocyte-derived cells into the resident pool. Importantly, these monocyte-derived resident cells are functionally different to their embryonic-

derived counterparts [14]. Therefore, it is possible that the protective effect of monocytes is exerted at the level of monocyte-derived, F4/80^{high} Tim4-ve resident cells. In this case, the reason why we do not observe notable differences during the early stages of the adhesion process may be due to the delay necessitated by the differentiation process of these cells.

Overall, our data suggest that several macrophage populations possess the capacity to prevent adhesion formation, with each acting at different phases of the resolution process (eg. resident cells early versus. monocyte-derived cells later) and utilising different, non-redundant mechanisms (eg. barrier-function versus fibrinolysis), respectively. Importantly, the effectiveness of these mechanisms is likely to be further influenced by other factors including severity of the injury [31], the presence of inflammatory stimuli [33] or neutrophil infiltration [11] as well as a possible genetic differences as shown here. Further research is required to identify conclusively the specific phenotype of monocyte-derived cells harbouring this protective capacity as well as to decipher their pivotal mechanism of action. Such data will allow the development of an innovative approach in preventing peritoneal adhesion maturation by modulating monocyte-derived macrophages following surgery.

Acknowledgements

The authors acknowledge funding from Medical Research Council (MRC) UK grant awarded to ASW, JA, DR, and SEH (MR/S02560X/1) and MRC UK grant (MR/P02615X/1) awarded to DR. We would like to thank John Grainger and Kara Filbey for providing the *Ccr2*-deficient mice. We would also like to thank Gareth Howell from the flow cytometry facility, staff in the Bioimaging facility and BSF facility at the University of Manchester, and Stella Pearson for technical assistence sectioning histology samples.

Author Contributions

RS: designed and performed experiments, analyzed data, and wrote the manuscript. KD: perfomed the surgery and edited the manuscript. DR and SH: designed experiments, analyzed data, and wrote

the manuscript. ASW and JA: designed experiments, provided input for interpretation and edited the manuscript. MM: provided input for interpretation and edited the manuscript.

Ethics statement

All animal experiments were approved by the University of Manchester Animal Welfare and Ethical Review Board and performed under the regulation of the Home Office Scientific Procedures Act (1986) and the Home Office approved licence (P1208AD89).

Availability of data and material

All data sets supporting this study are available on request.

References

1. Tang J, Xiang Z, Bernards MT, *et al.* Peritoneal adhesions: occurrence, prevention and experimental models. Acta Biomater 2020;116:84-104.
2. Herrick SE, Allen JE. Surgical adhesions: A sticky macrophage problem. Science 2021;371(6533):993-4
3. Ryan GB, Grobéty J, Majno G. Postoperative peritoneal adhesions: a study of the mechanisms. Am J Pathol 1971;65(1):117.
4. Brokelman WJ, Holmdahl L, Janssen IM, *et al.* Decreased peritoneal tissue plasminogen activator during prolonged laparoscopic surgery. J Surg Res 2009;151(1):89-93.
5. Tsai JM, Sinha R, Seita J, *et al.* Surgical adhesions in mice are derived from mesothelial cells and can be targeted by antibodies against mesothelial markers. Sci Transl Med 2018;10(469):eaan6735.
6. Sandoval P, Jiménez-Heffernan JA, Guerra-Azcona G, *et al.* Mesothelial-to-mesenchymal transition in the pathogenesis of post-surgical peritoneal adhesions. J Pathol 2016;239(1):48-59.
7. Kubicka U, Olszewski W, Tarnowski W, *et al.* Normal human immune peritoneal cells: subpopulations and functional characteristics. Scand J Immunol 1996;44(2):157-63.
8. Burnett SH, Beus BJ, Avdiushko R, *et al.* Development of peritoneal adhesions in macrophage depleted mice. J Surg Res 2006;131(2):296-301.
9. Ar'Rajab A, Dawidson I, Sentementes J, *et al.* Enhancement of peritoneal macrophages reduces postoperative peritoneal adhesion formation. J Surg Res 1995;58(3):307-12.
10. Hoshino A, Kawamura YI, Yasuhara M, *et al.* Inhibition of CCL1-CCR8 interaction prevents aggregation of macrophages and development of peritoneal adhesions. J Immunol 2007;178(8):5296-304.
11. Tsai JM, Shoham M, Fernhoff NB, *et al.* Neutrophil and monocyte kinetics play critical roles in mouse peritoneal adhesion formation. Blood Adv 2019;3(18):2713-21.
12. Honjo K, Munakata S, Tashiro Y, *et al.* Plasminogen activator inhibitor-1 regulates macrophage-dependent postoperative adhesion by enhancing EGF-HER1 signaling in mice. The FASEB J 2017;31(6):2625-37.
13. Cassado AdA, D'Império Lima MR, Bortoluci KR. Revisiting mouse peritoneal macrophages: heterogeneity, development, and function. Front Immunol 2015;6:225.
14. Louwe P, Badiola Gomez L, Webster H, *et al.* Recruited macrophages that colonize the post-inflammatory peritoneal niche convert into functionally divergent resident cells. Nat Commun 2021;12(1):1-15.
15. Ghosn EEB, Cassado AA, Govoni GR, *et al.* Two physically, functionally, and developmentally distinct peritoneal macrophage subsets. Proc Nat Acad Sci 2010;107(6):2568-73.
16. Bain CC, Jenkins SJ. The biology of serous cavity macrophages. Cell Immunol 2018;330:126-35.
17. Campbell SM, Knipper JA, Ruckerl D, *et al.* Myeloid cell recruitment versus local proliferation differentiates susceptibility from resistance to filarial infection. Elife. 2018;7:e30947.
18. Finlay CM, Parkinson JE, Chan BH, *et al.* Genotype and Th2 cells control monocyte to tissue resident macrophage differentiation during nematode infection of the pleural cavity. Available at SSRN 3992680. 2021.
19. Sulaiman H, Gabella G, Davis C, *et al.* Growth of nerve fibres into murine peritoneal adhesions. J Pathol 2000;192(3):396-403.
20. Gorvy DA, Herrick SE, Shah M, *et al.* Experimental manipulation of transforming growth factor-β isoforms significantly affects adhesion formation in a murine surgical model. Am J Pathol 2005;167(4):1005-19.
21. Mack M, Cihak J, Simonis C, *et al.* Expression and characterization of the chemokine receptors CCR2 and CCR5 in mice. J Immunol 2001;166(7):4697-704.
22. Molinas CR, Binda MM, Campo R, *et al.* Adhesion formation and interanimal variability in a laparoscopic mouse model varies with strains. Fertil Steril 2005;83(6):1871-4.

23. Bain CC, Hawley CA, Garner H, *et al.* Long-lived self-renewing bone marrow-derived macrophages displace embryo-derived cells to inhabit adult serous cavities. Nat Commun 2016;7(1):1-14.
24. Ito T, Shintani Y, Fields L, *et al.* Cell barrier function of resident peritoneal macrophages in post-operative adhesions. Nat Commun 2021;12(1):1-12.
25. Bain C, Gibson D, Steers N, *et al.* Rate of replenishment and microenvironment contribute to the sexually dimorphic phenotype and function of peritoneal macrophages. Sci Immunol 2020;5(48):eabc4466.
26. Takenaka E, Van Vo A, Yamashita-Kanemaru Y, *et al.* Selective DNAM-1 expression on small peritoneal macrophages contributes to CD4+ T cell costimulation. Sci Rep 2018;8(1):1-8.
27. Liao CT, Rosas M, Davies LC, *et al.* IL-10 differentially controls the infiltration of inflammatory macrophages and antigen-presenting cells during inflammation. Eur J Immunol 2016;46(9):2222-32.
28. Meda C, Molla F, De Pizzol M, *et al.* Semaphorin 4A exerts a proangiogenic effect by enhancing vascular endothelial growth factor-A expression in macrophages. J Immunol 2012;188(8):4081-92.
29. Tsou C-L, Peters W, Si Y, *et al.* Critical roles for CCR2 and MCP-3 in monocyte mobilization from bone marrow and recruitment to inflammatory sites. J Clin Invest 2007;117(4):902-9.
30. Rückerl D, Campbell SM, Duncan S, *et al.* Macrophage origin limits functional plasticity in helminth-bacterial co-infection. PLoS Pathog 2017;13(3):e1006233.
31. Zindel J, Peiseler M, Hossain M, *et al.* Primordial GATA6 macrophages function as extravascular platelets in sterile injury. Science 2021;371(6533).
32. Vega-Pérez A, Villarrubia LH, Godio C, *et al.* Resident macrophage-dependent immune cell scaffolds drive anti-bacterial defense in the peritoneal cavity. Immun 2021;54(11):2578-94. e5.
33. Zindel J, Mittner J, Bayer J, *et al.* Intraperitoneal microbial contamination drives post-surgical peritoneal adhesions by mesothelial EGFR-signaling. Nat Commun 2021;12(1):1-17.

Figure legends

Figure 1. BALB/c mice showed more peritoneal adhesions than C57BL/6 mice at day 14 post-surgery (p.s.), and fewer monocytes and macrophages at day 3. Adhesion scores after surgery at different time points. (A) Representative image and corresponding histological appearance (Masson's trichrome staining) of adhesions between mouse strains at day 14 after surgery. (B) Collagen analysis in adhesion histological sections at day 14. (C) Total cell number of total peritoneal cavity macrophages (D), peritoneal resident macrophages (E), monocytes (F), peritoneal F4/80^{low} macrophages (G) and peritoneal F4/80^{int} intermediate macrophages (H). Data shows mean±SEM, pooled from 6 separate experiments for naïve or 2 separate experiments for day 3, 7, and 14 post-surgery., n= 6 - 20 mice/group; *P<0.05, **P<0.01, ***P<0.001, ****P<0.0001. (A and C) Mann Whitney test and (D-H) ANOVA with Tukey's multiple comparison test.

Figure 2. Peritoneal macrophage markers and cytokine profiles post-surgery in BALB/c mice were altered compared with C57BL/6 mice. Relative % of CD102+ (A), Gata6+ (B), and Tim4+ (C) of F4/80^{high} population. Relative % of CD226+ (D), Sema4a+ (E), and Lyve1+ (F) of F4/80^{low} macrophage population. Total cell number of Sca1+ (G), Relmα+ (H), and Ym1+ (I) in myeloid cells (CD11b+lin-Ly6C- cells)/total peritoneal cavity macrophages by flow cytometry. Peritoneal lavage levels for Relmα (J) and Ym1 (K) by ELISA. Data shows mean±SEM, pooled from 6 separate experiments for naïve or 2 separate experiments for day 3, 7, and 14 p.s., n= 6 - 20 mice/group; *P<0.05, **P<0.01, ****P<0.0001, ANOVA with Tukey's multiple comparison test.

Figure 3. *Ccr2*-deficient mice were more susceptible to peritoneal adhesion formation post-surgery compared with their WT littermates. Adhesion scores (A) and representative adhesion image at day 7 after surgery. (B). Relative percentage of peritoneal F4/80^{high} resident macrophages (C), monocytes (D), peritoneal F4/80^{low} monocyte-derived macrophages (E), and peritoneal F4/80^{int} macrophages (F). Total cell number of peritoneal F4/80^{high} resident macrophages (G), monocytes (H),

peritoneal F4/80^{low} monocyte-derived macrophages (I), and peritoneal F4/80^{int} macrophages (J). Data shows mean±SEM, pooled from 4 separate experiments for naïve or 3 separate experiments for day 7, n= 4 - 6 mice/group; all females for day 7 but mixed male and female for naive; *P<0.05, **P<0.01, (A) Mann Whitney test, (C-J) ANOVA with Tukey's multiple comparison test.

Figure 4. Macrophages markers associated with monocyte-derived and intermediate subsets were altered in *Ccr2*-deficient mice. Relative % of Tim+ (A) within F4/80^{high} population, Relative % of Sema4a+ within F4/80^{low} (B), F4/80^{int} (C), and F4/80^{high} (D). Relative % of Lyve1+ within F4/80^{low} (E), F4/80^{int} (F), and F4/80^{high} (G). Relative % of CD226+ within F4/80^{low} (H). Total number of CD226+ cells within F4/80^{low} subset (I) Total number of CD206+ (J) and Relmα+ (K) cells within total peritoneal macrophages. Cytokine level of Relmα in peritoneal lavage (L) using ELISA. Data shows mean±SEM, pooled from 4 separate experiments for naïve or 3 separate experiments for day 7, n= 4 - 6 mice/group; all females for day 7 but mixed male and female for naive, *P<0.05, **P<0.01, ***P<0.001, ****P<0.0001, ANOVA with Tukey's multiple comparison test.

Figure 5. Depletion of monocyte-derived peritoneal macrophages enhanced susceptibility of C57BL/6 mice to peritoneal adhesions post-surgery. Schematic of experiment approach (A). Adhesion score at day 14 (B). Representative image and corresponding histological appearance (Masson's trichrome staining) of adhesions at day 14 in mice treated with CCR2-mAb or control IgG2b (C). Collagen analysis in adhesion histological sections at day 14 (D). Total peritoneal exudate cells (E). Total cell number of peritoneal F4/80^{high} resident macrophages (F) and monocytes (G) at day 3 and 14 post-surgery. Relative % of Tim4+ cells within F4/80^{high} population (H). Level of Relmα in peritoneal lavage at day 14 (I). Data shows mean±SEM, pooled from 2 separate experiments, n= 6 - 8 mice/group; *P<0.05, **P<0.01, ****P<0.0001; (B, D, I) Mann Whitney test, (E-H) ANOVA with Tukey's multiple comparison test.

Figure 6. Monocytes and/or monocyte-derived peritoneal macrophages are essential in preventing peritoneal adhesion formation after surgery. BALB/c mice had a significantly lower influx of monocytes and monocyte-derived macrophages at day 3 post-surgery, leading to greater peritoneal adhesion formation at day 14 post-surgery (A) compared with C57BL/6 mice (B). Blocking the recruitment of circulating monocytes in C57BL/6 mice resulted in an enhanced susceptibility to peritoneal adhesions after surgery (C).

List of Supplementary Material

Supplementary Table 1. Adhesion scoring system

Supplementary Table 2. Panel 1 flow cytometry

Supplementary Table 3. Panel 2 flow cytometry

Supplementary Table 4. The coating and detection antibody for ELISA

Supplementary Figure 1. Gating strategy for flow cytometry analysis of PECs with the representative of lineage+ lineage- and F4/80 against IA/IE plots between BALB/c and C57BL/6 mice prior and after surgery.

Supplementary Figure 2. Representative of adhesion images and Masson's trichrome staining and total collagen at day 3 and 7 post-surgery between BALB/c and C57BL/6 mice.

Supplementary Figure 3. Peritoneal exudate cells and relative percentage of peritoneal macrophages and monocytes prior and after surgery.

Supplementary Figure 4. Relative percentages for different markers expressed by peritoneal macrophages within BALB/c and C57BL/6 mice prior and post-surgery.

Supplementary Figure 5. Schematic representation of how different markers of peritoneal macrophages were expressed in different subsets.

Supplementary Figure 6. Cytokine analysis in the peritoneal lavage of BALB/c and C57BL/6 before and after surgery.

Supplementary Figure 7. Cytokine analysis in the peritoneal lavage of *Ccr2*KO and WT littermate before and after surgery.

Supplementary Figure 8. Relative percentage of monocytes and different markers of peritoneal macrophages of Rat IgG2b isotype control and anti-CCR2 (clone MC21) treated mice after surgery.

Supplementary Figure 9. Total cell number of monocytes and different markers of peritoneal macrophages of Rat IgG2b isotype control and anti-CCR2 (clone MC21) antibody treated mice after surgery.

Supplementary Figure 10. Cytokine analysis in the peritoneal lavage of Rat IgG2b isotype control and anti-CCR2 (clone MC21) antibody treated mice after surgery.

Supplementary Figure 11. The relative percentage and total cell number of neutrophils in the peritoneal cavity of BALB/c and C57BL/6 mice prior and after surgery.

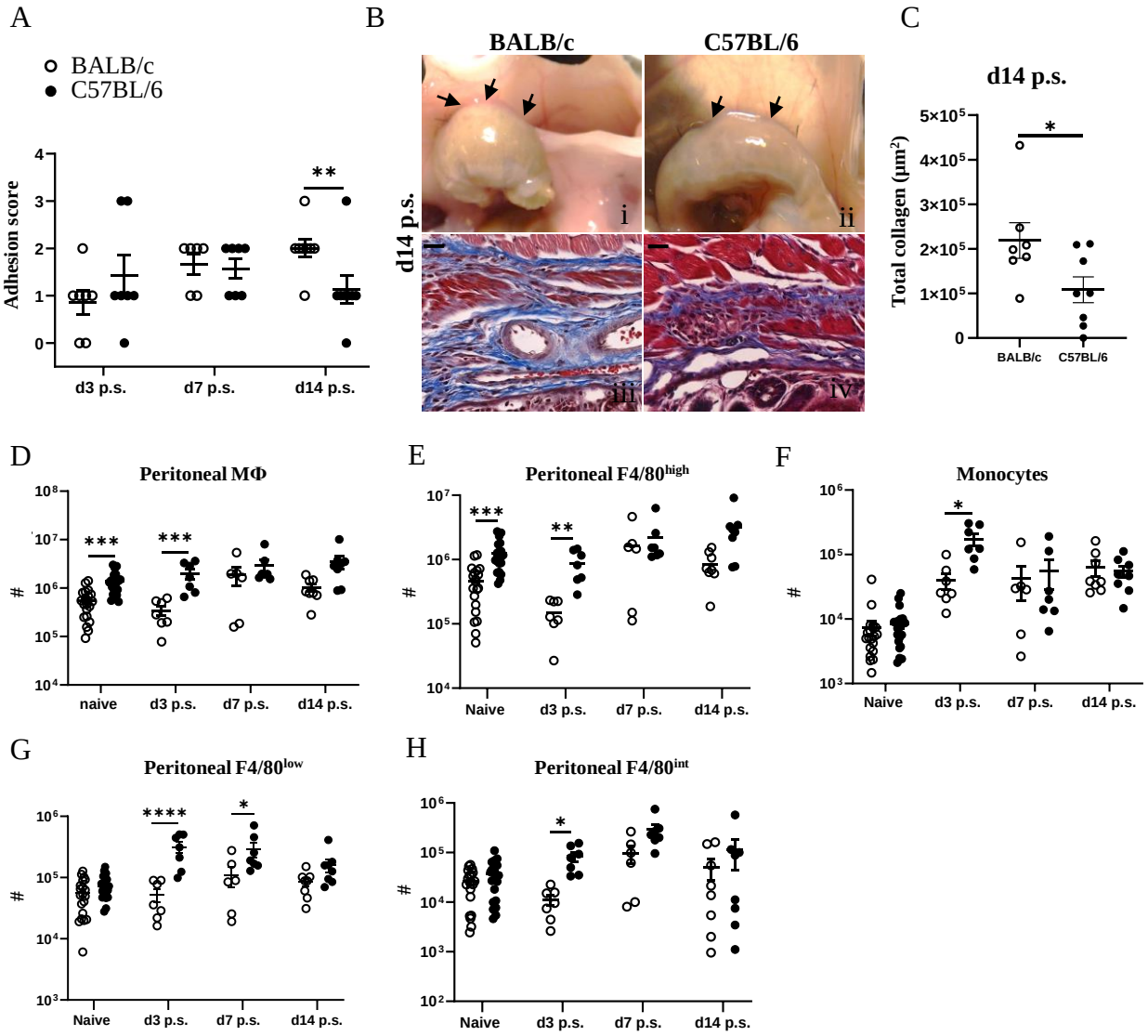
A
BALB/c
C57BL/6
Adhesion score
d3 p.s.
d7 p.s.
d14 p.s.
**
B
BALB/c
C57BL/6
d14 p.s.
i
ii
iii
iv
C
d14 p.s.
Total collagen (µm²)
BALB/c
C57BL/6
*
D
Peritoneal MΦ
#
naive
d3 p.s.
d7 p.s.
d14 p.s.
***
***
E
Peritoneal F4/80high
Naive
d3 p.s.
d7 p.s.
d14 p.s.
***
**
F
Monocytes
Naive
d3 p.s.
d7 p.s.
d14 p.s.
*
G
Peritoneal F4/80low
Naive
d3 p.s.
d7 p.s.
d14 p.s.
****
*
H
Peritoneal F4/80int
Naive
d3 p.s.
d7 p.s.
d14 p.s.
*

Figure 1.

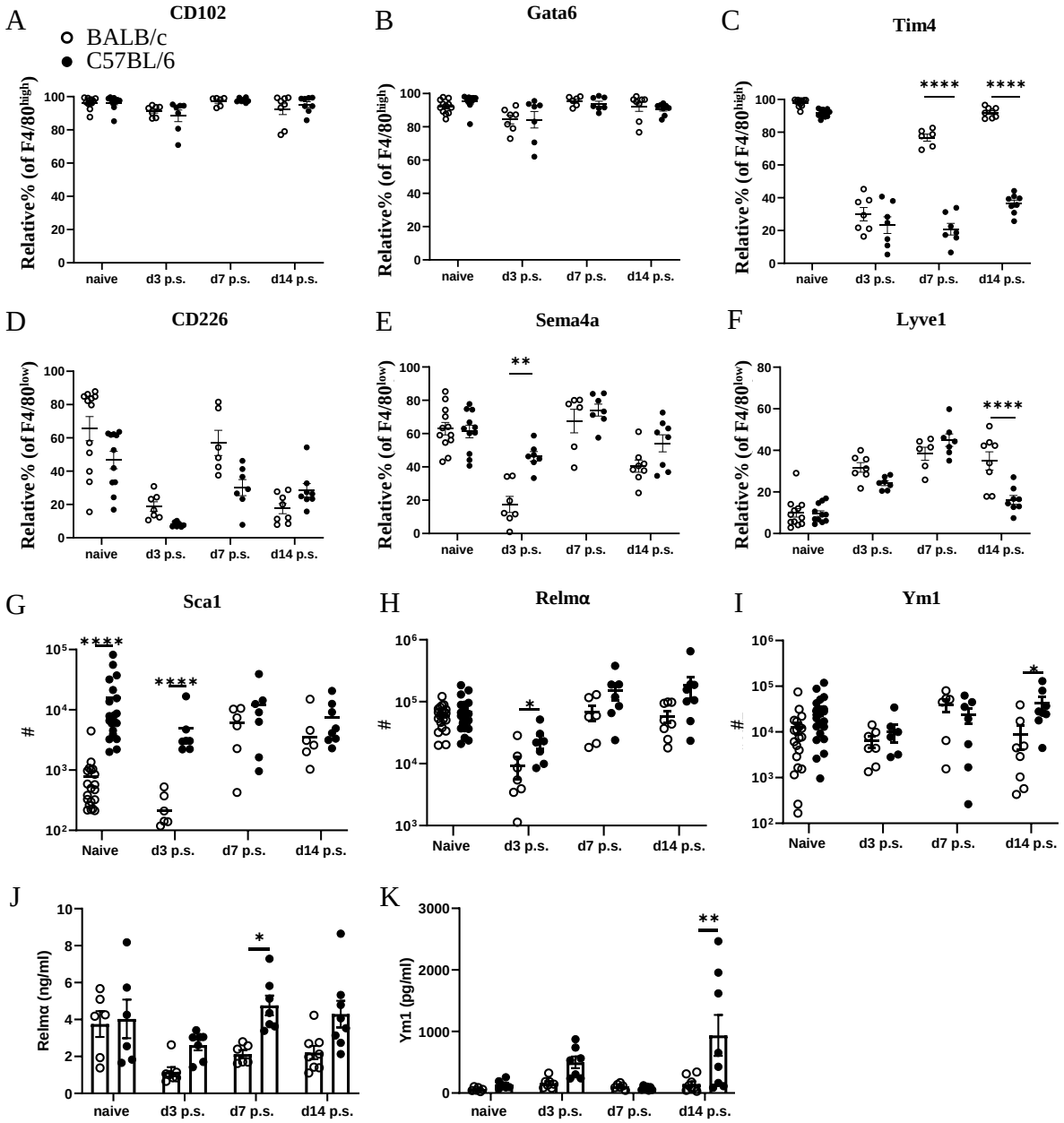
A
CD102
BALB/c
C57BL/6
Relative% (of F4/80high)
naive
d3 p.s.
d7 p.s.
d14 p.s.
B
Gata6
C
Tim4
****
****
D
CD226
Relative% (of F4/80low)
E
Sema4a
**
F
Lyve1
****
G
Sca1
****
****
#
Naive
H
Relmα
*
I
Ym1
*
J
Relmα (ng/ml)
*
K
Ym1 (pg/ml)
**

Figure 2.

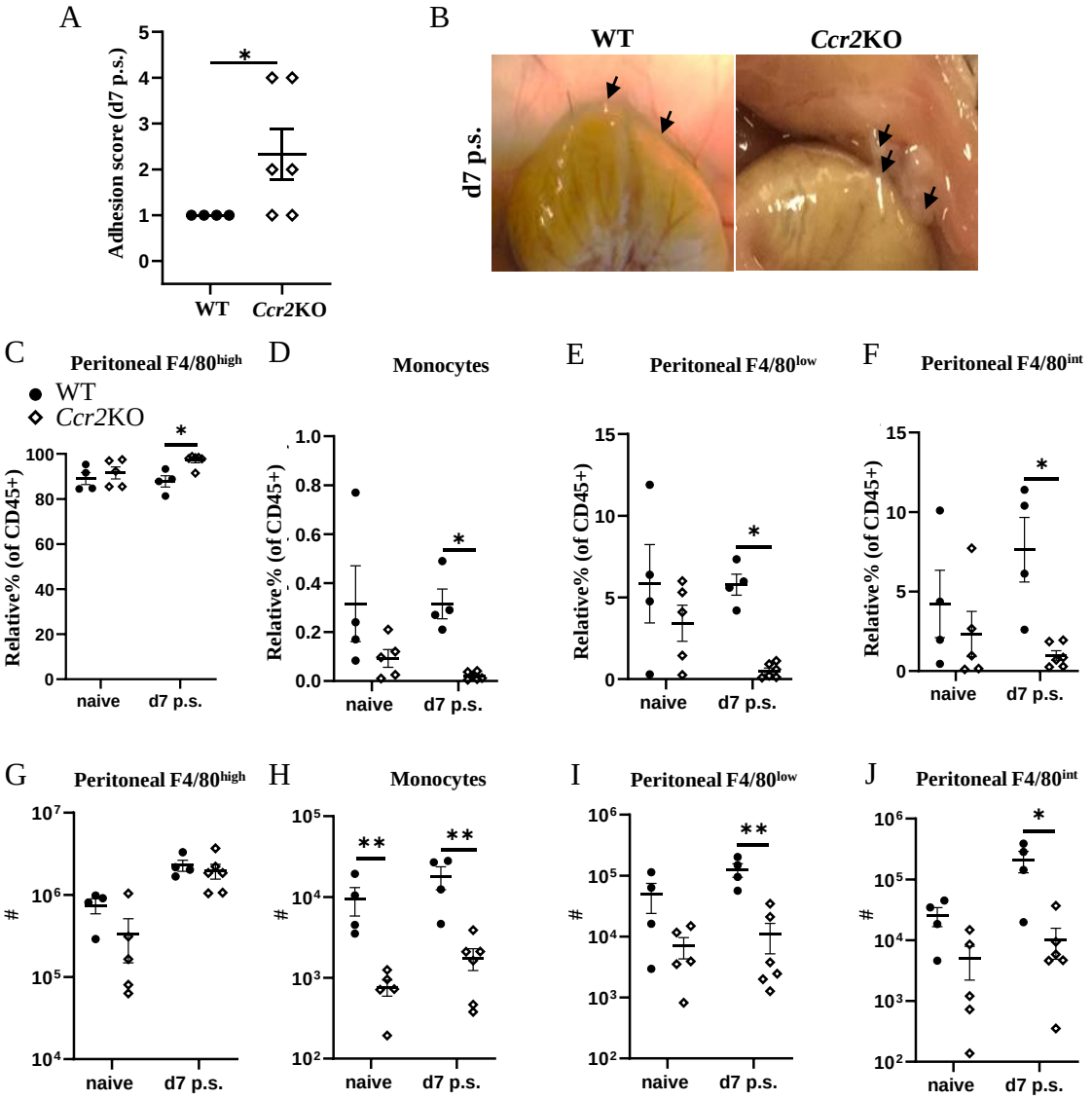
A
Adhesion score (d7 p.s.)
WT
Ccr2KO
B
WT
Ccr2KO
d7 p.s.
C
Peritoneal F4/80high
WT
Ccr2KO
Relative% (of CD45+)
naive
d7 p.s.
D
Monocytes
E
Peritoneal F4/80low
F
Peritoneal F4/80int
G
Peritoneal F4/80high
#
H
Monocytes
I
Peritoneal F4/80low
J
Peritoneal F4/80int

Figure 3.

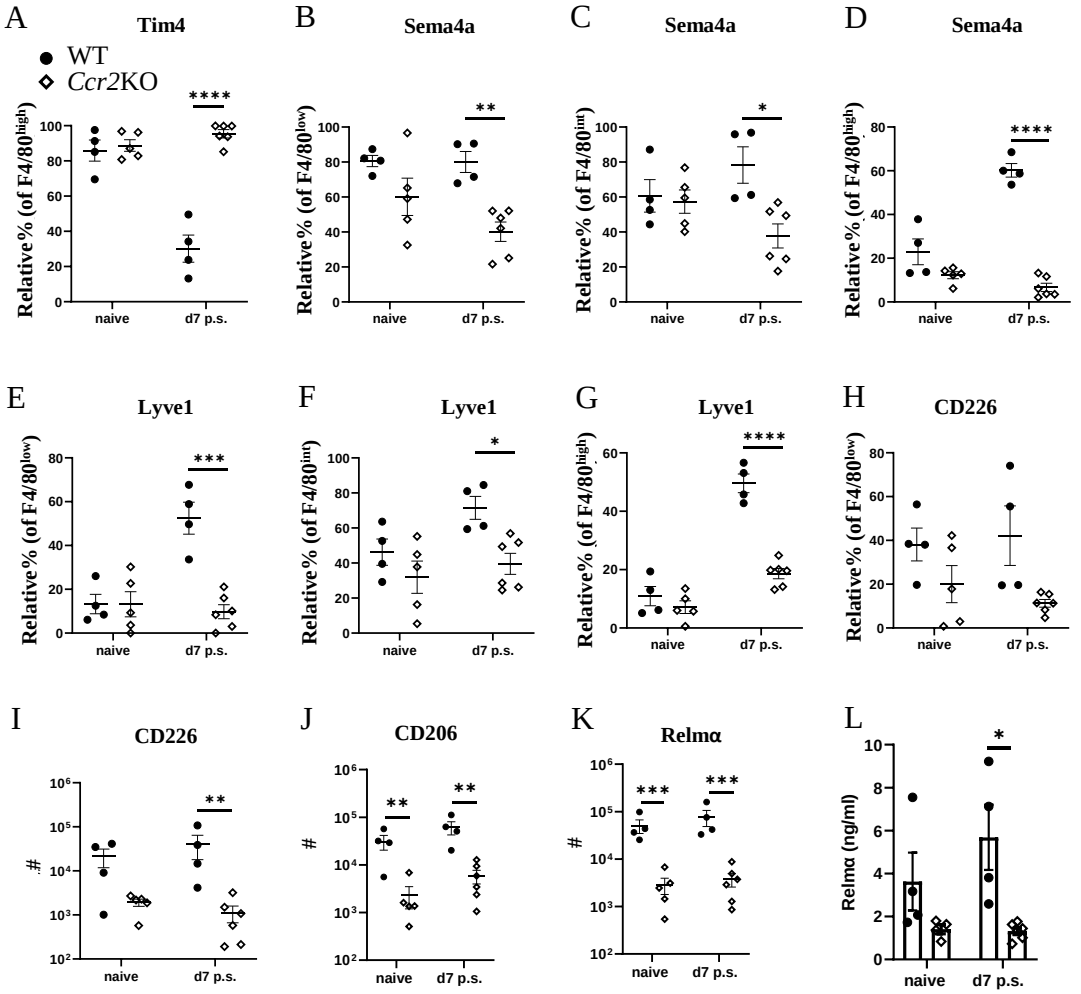
A
Tim4
WT
Ccr2KO
Relative% (of F4/80high)
naive
d7 p.s.
B
Sema4a
Relative% (of F4/80low)
C
Sema4a
Relative% (of F4/80int)
D
Sema4a
E
Lyve1
Relative% (of F4/80low)
F
Lyve1
Relative% (of F4/80int)
G
Lyve1
H
CD226
Relative% (of F4/80low)
I
CD226
#
J
CD206
#
K
Relmα
#
L
Relmα (ng/ml)

Figure 4.

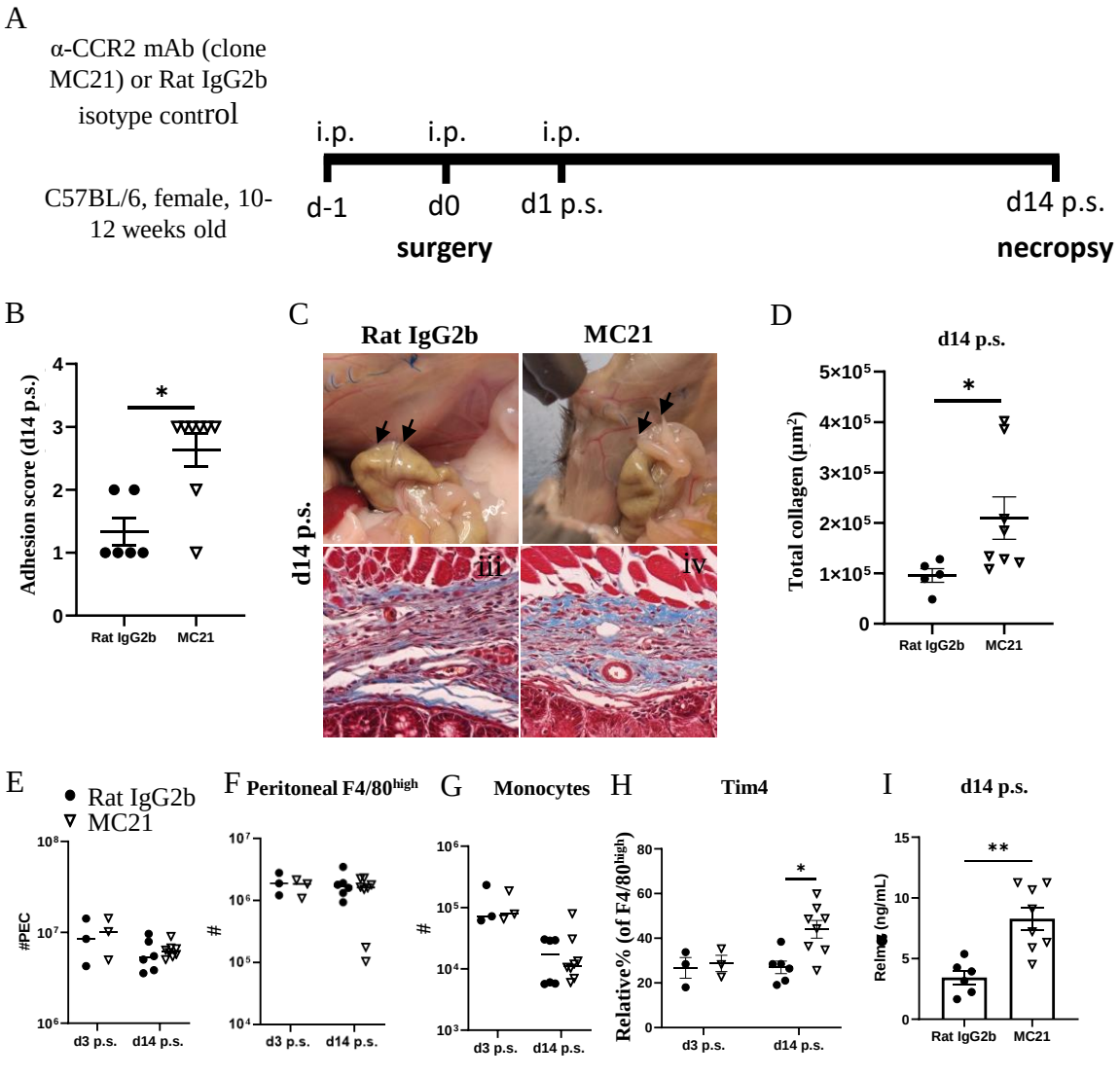
A
α-CCR2 mAb (clone MC21) or Rat IgG2b isotype control
C57BL/6, female, 10-12 weeks old
i.p.
i.p.
i.p.
d-1
d0
d1 p.s.
d14 p.s.
surgery
necropsy
B
Adhesion score (d14 p.s.)
Rat IgG2b
MC21
C
Rat IgG2b
MC21
d14 p.s.
iii
iv
D
d14 p.s.
Total collagen (μm²)
Rat IgG2b
MC21
E
Rat IgG2b
MC21
#PEC
d3 p.s.
d14 p.s.
F Peritoneal F4/80high
#
d3 p.s.
d14 p.s.
G Monocytes
#
d3 p.s.
d14 p.s.
H Tim4
Relative% (of F4/80high)
d3 p.s.
d14 p.s.
I d14 p.s.
Relmα (ng/mL)
Rat IgG2b
MC21

Figure 5.

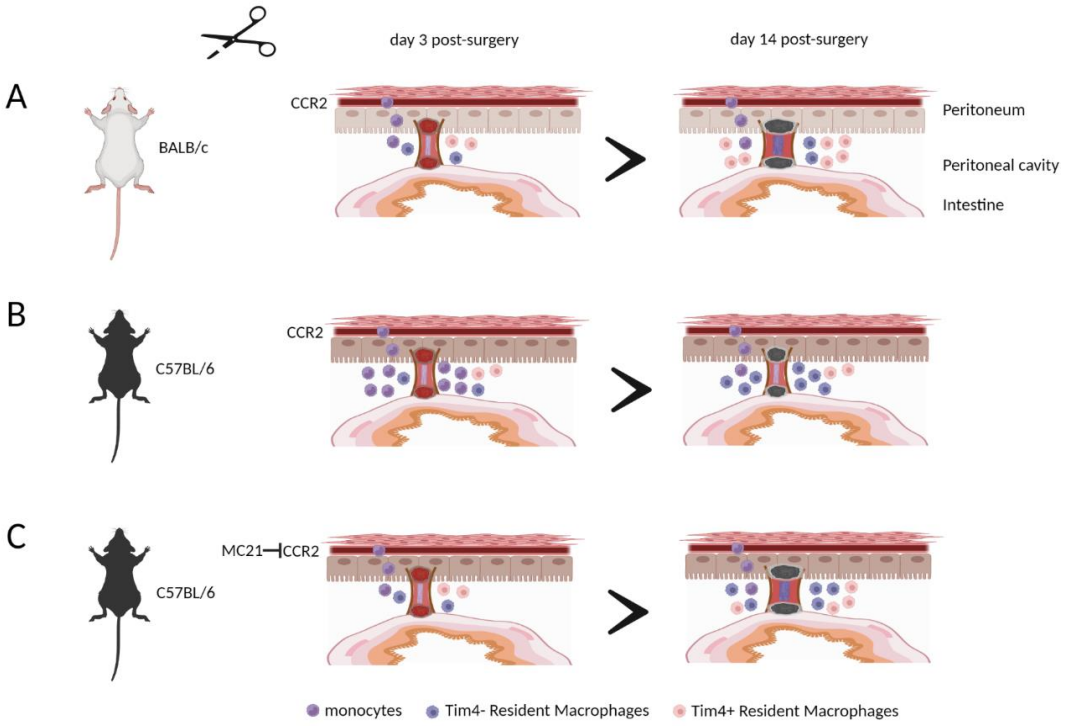

Created with BioRender.com

Figure 6.

Supplementary Table 1. Adhesion scoring system.

Adhesion						
No adhesion **(Cat: 0)**	**Injured peritoneum**			**Incision site**		
	Caecum to injured peritoneum **(Cat:1)**	Pelvic fat to injured peritoneum/caecum **(Cat: 2)**	Omentum to injured peritoneum/caecum **(Cat: 2)**	Pelvic fat to incision site **(Cat: 3)**	Omentum to incision site **(Cat: 3)**	Organ(s) to incision site/injury site **(Cat: 4)**

Cat:0

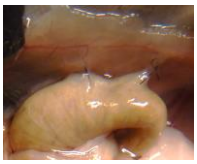

Cat:1

Cat:2

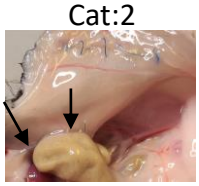

Cat:3

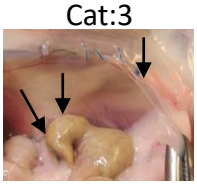

Cat:4

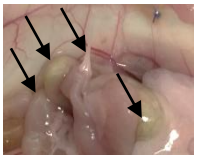

Cat: Category

Supplementary Table 2. Panel 1 flow cytometry

Filter	Channel	Antigen	Clone	Supplier
355 450_50	BUV440	Live/Dead	Zombie UV	Biolegend
355 735_30	BUV737	Ym1 biotin	BAF2446	R& D System
405 450_50	PB	CD19	6D5	Biolegend
405 450_50	BV421	SigF	S17007L	Biolegend
405 450_50	PB	TCRβ	H57-597	Biolegend
405 450_50	PB	Ly6G	1A8	Biolegend
405 450_50	BV421	NK1.1	PK136	Biolegend
405 450_50	BV421	Ter119	TER-119	Biolegend
405 525_50	BV510	Ly6C	HK1.4	Biolegend
405 605_40	BV605	CD11c	N418	Biolegend
405 677_20	BV650	CD102	3C4(mIC2/4)	BD Biosciences
405 710_50	BV711	CD11b	M1/70	Biolegend
405 750_30	BV750-P	TNFa	MP6-XT22	Biolegend
405 810_40	BV786	Sca-1	D7	Biolegend
488 530_30	AF488	Relm-a	500-P214-100	Peprotech
488 710_50	PerCPeF 710	CD73	eBioTY/11.8	Invitrogen
561 586_15	PE	GATA6	D61E4	Cell Signaling Technology
561 610_20	PE-CF594	F4/80	BM8	Biolegend
561 670_30	PE-Cy5	CD45	30-F11	Biolegend
561 780_60	PE-Cy7	Tim4	RMT4-54	Biolegend
637 670_30	AF647	CD115	AFS98	Biolegend
637 730_45	AF700	I-A/I-E	M5/114.15.2	Biolegend
637 780_60	APC-cy7	CD226	10E5	Biolegend

Supplementary Table 3. Panel 2 flow cytometry

Filter	Channel	Antigen	Clone	Suplier
355 450_50	BUV440	Live/Dead	Zombie UV	Biolegend
355 735_30	BUV737	CD206 biotin	C068C2	Biolegend
405 450_50	PB	CD19	6D5	Biolegend
405 450_50	BV421	SigF	S17007L	Biolegend
405 450_50	PB	TCRβ	H57-597	Biolegend
405 450_50	PB	Ly6G	1A8	Biolegend
405 450_50	BV421	NK1.1	PK136	Biolegend
405 450_50	BV421	Ter119	TER-119	Biolegend
405 525_50	BV510	Ly6C	HK1.4	Biolegend
405 605_40	BV605	CD11c	N418	Biolegend
405 677_20	BV650	CD102	3C4(mIC2/4)	BD Biosciences
405 710_50	BV711	CD11b	M1/70	Biolegend
405 810_40	BV786	Ki76	B56	BD Biosciences
488 530_30	AF488	Relma	500-P214-100	Peprotech
488 710_50	PerCPeF 710	CD73	eBioTY/11.8	Invitrogen
561 586_15	PE	Lyve-1	10/FR2	Biolegend
561 610_20	PE-CF594	F4/80	BM8	Biolegend
561 670_30	PE-Cy5	CD45	30-F11	Biolegend
561 780_60	PE-Cy7	Tim4	RMT4-54	Biolegend
637 670_30	AF647	sema4a	5E3/SEMA4A	Biolegend
637 730_45	AF700	I-A/I-E	M5/114.15.2	Biolegend
637 780_60	APC-cy7	CD115	AFS98	Biolegend

Supplementary Table 4. The coating and detection antibody for ELISA

Cytokine	Coating antibody clone	Supplier	Detection antibody clone	Supplier
IL-4	11B11	Biolegend	BVD6-24G2	Biolegend
IL-10	JES5-16E3	Biolegend	JES5-2A5	Biolegend
IL-13	eBio13A	Invitrogen	eBio1316H	Invitrogen
Relm-α	500-P214	Peprotech	500-P214Bt	Peprotech
Ym1	Duoset	R&D System	Duoset	R&D System
IFN-γ	Cat. 551216	BD Biosciences	XMG1.2	Biolegend
IL-12p40	C15.6	Biolegend	C17.8	Biolegend
IL-6	Cat. 554400	BD Biosciences	MP5-3C11	Biolegend
TNF-α	MP6-XT22	Biolegend	MP6-XT22	Biolegend

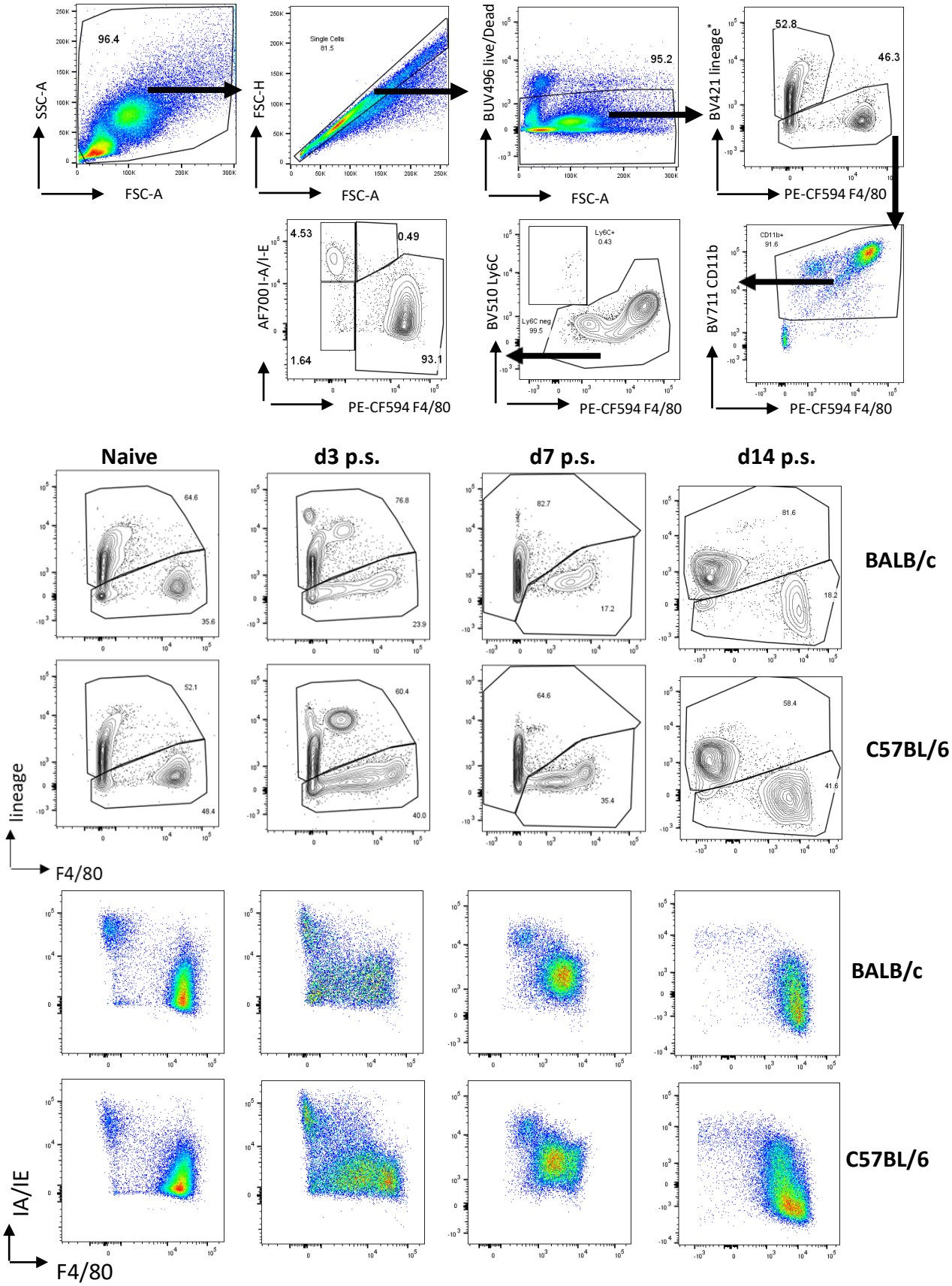

Supplementary Figure 1. Gating strategy for flow cytometry analysis of PECs with the representative of lineage+ lineage- and F4/80 against IA/IE plots between BALB/c and C57BL/6 mice prior and after surgery.

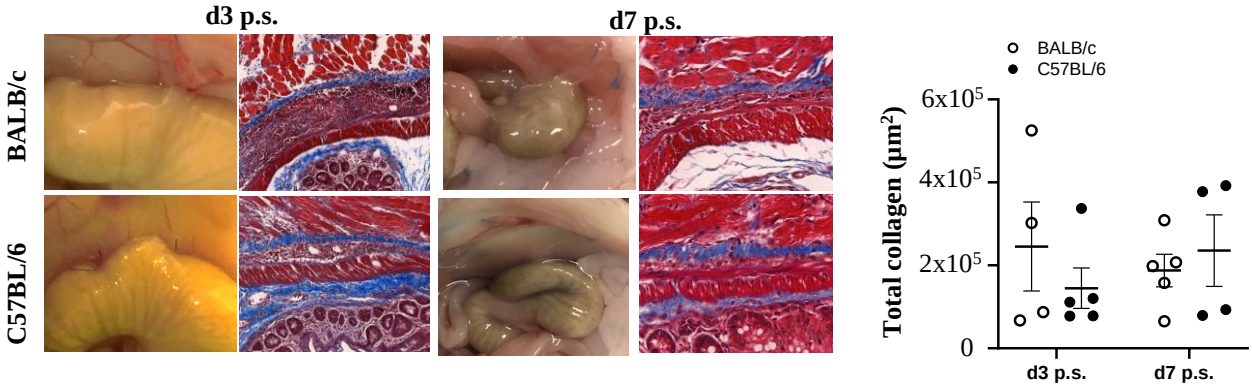

Supplementary Figure 2. Representative of adhesion images and Masson's trichrome staining and total collagen at day 3 and 7 post-surgery between BALB/c and C57BL/6 mice.

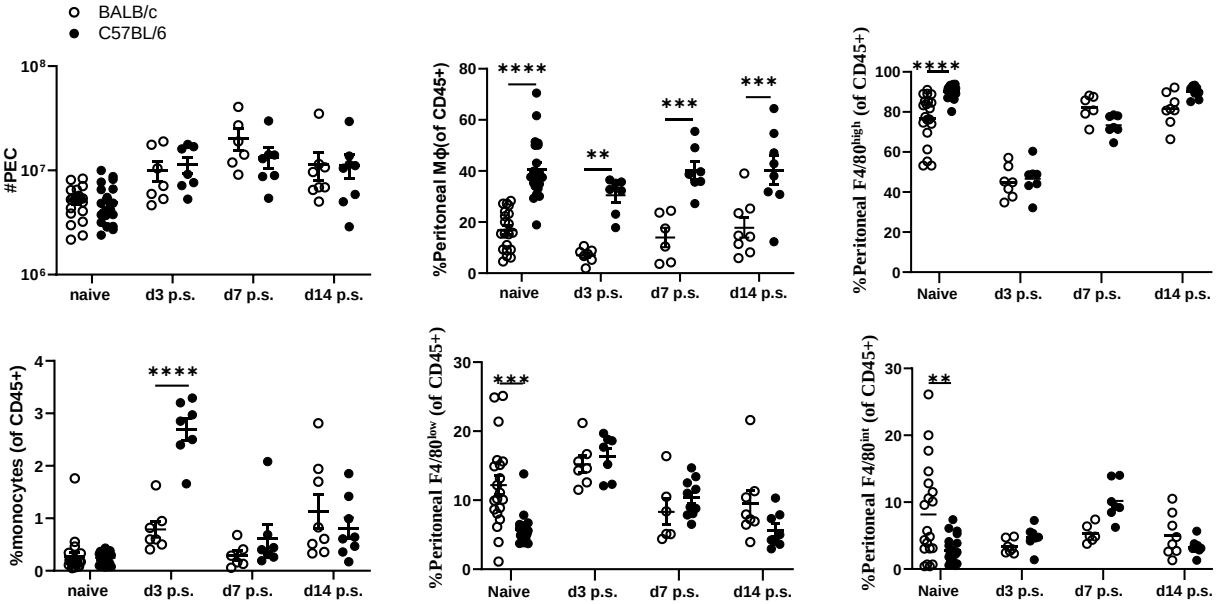

Supplementary Figure 3. Peritoneal exudate cells and relative percentage of peritoneal macrophages and monocytes prior and after surgery

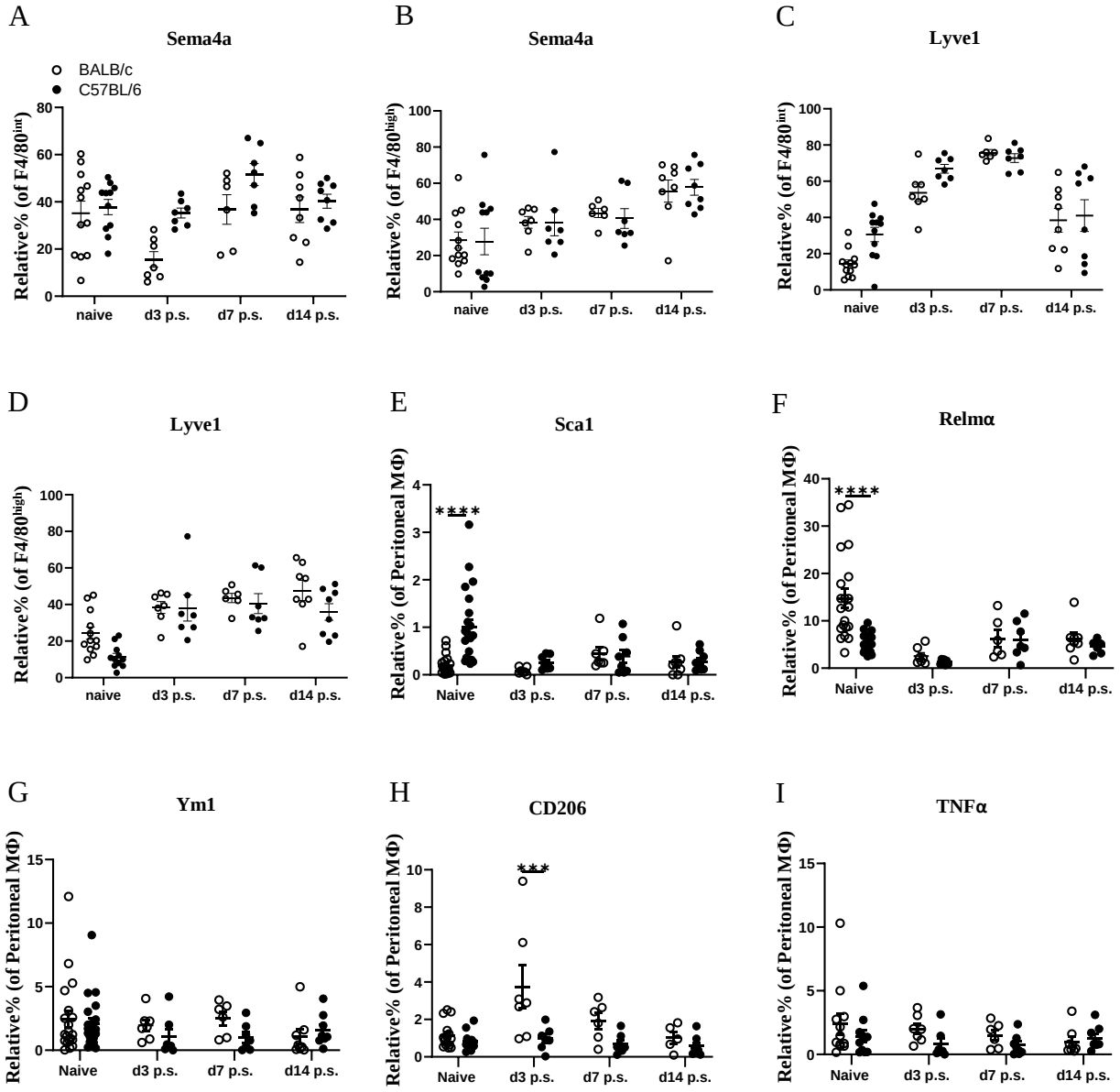

Supplementary Figure 4. Relative percentages for different markers expressed by peritoneal macrophages within BALB/c and C57BL/6 mice prior and post-surgery.

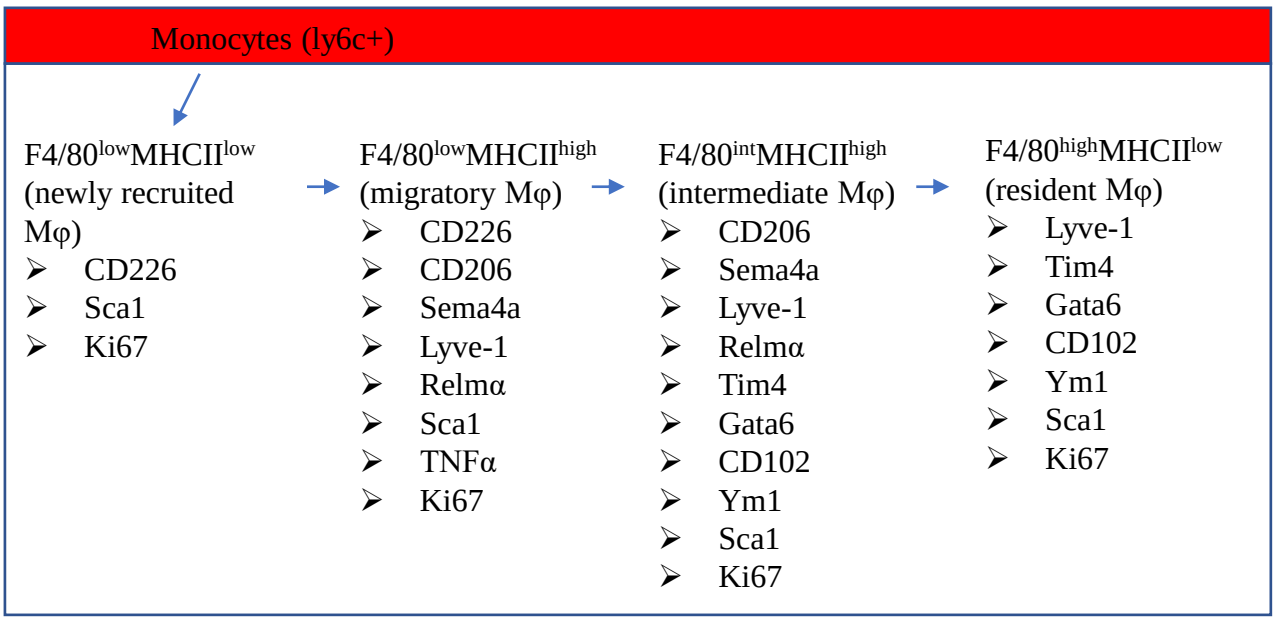

Supplementary Figure 5. Schematic representation of how different markers of peritoneal macrophages were expressed in different subsets

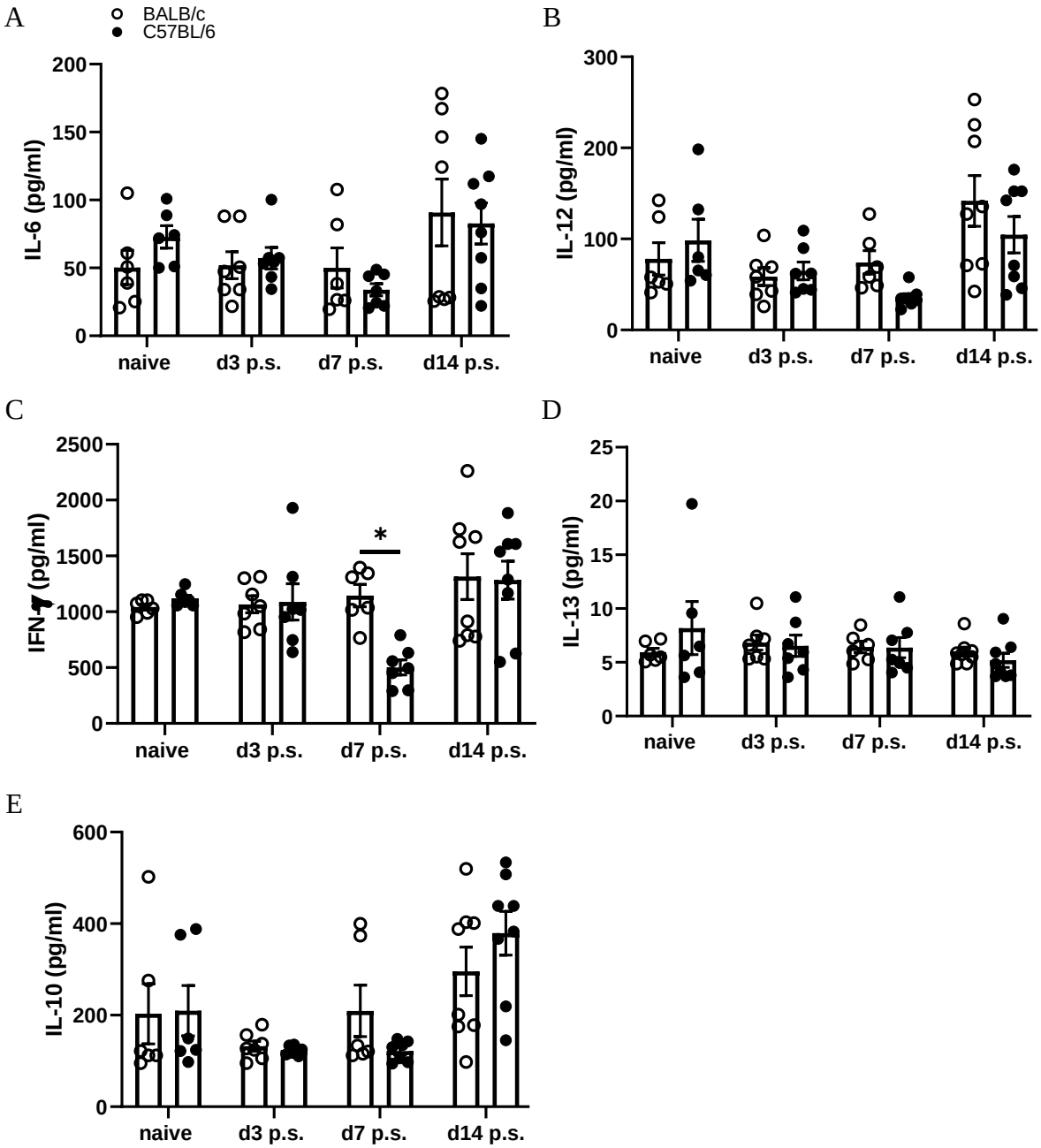

Supplementary Figure 6. Cytokine analysis in the peritoneal lavage of BALB/c and C57BL/6 before and after surgery.

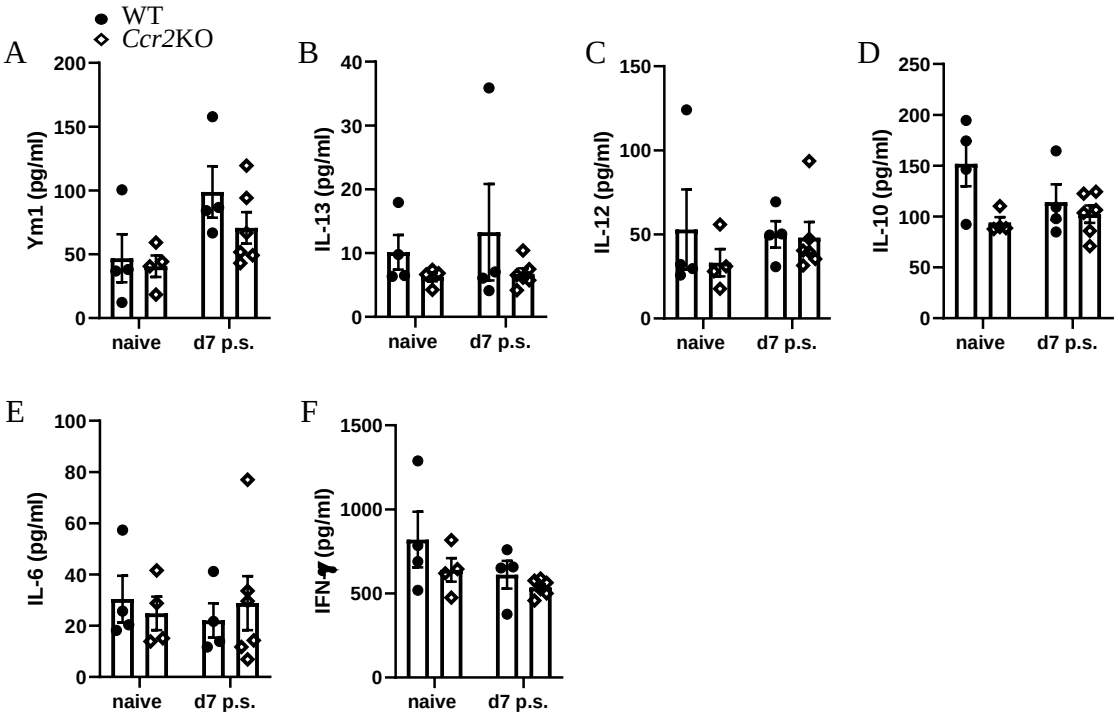

Supplementary Figure 7. Cytokine analysis in the peritoneal lavage of *Ccr2*KO and WT littermate before and after surgery.

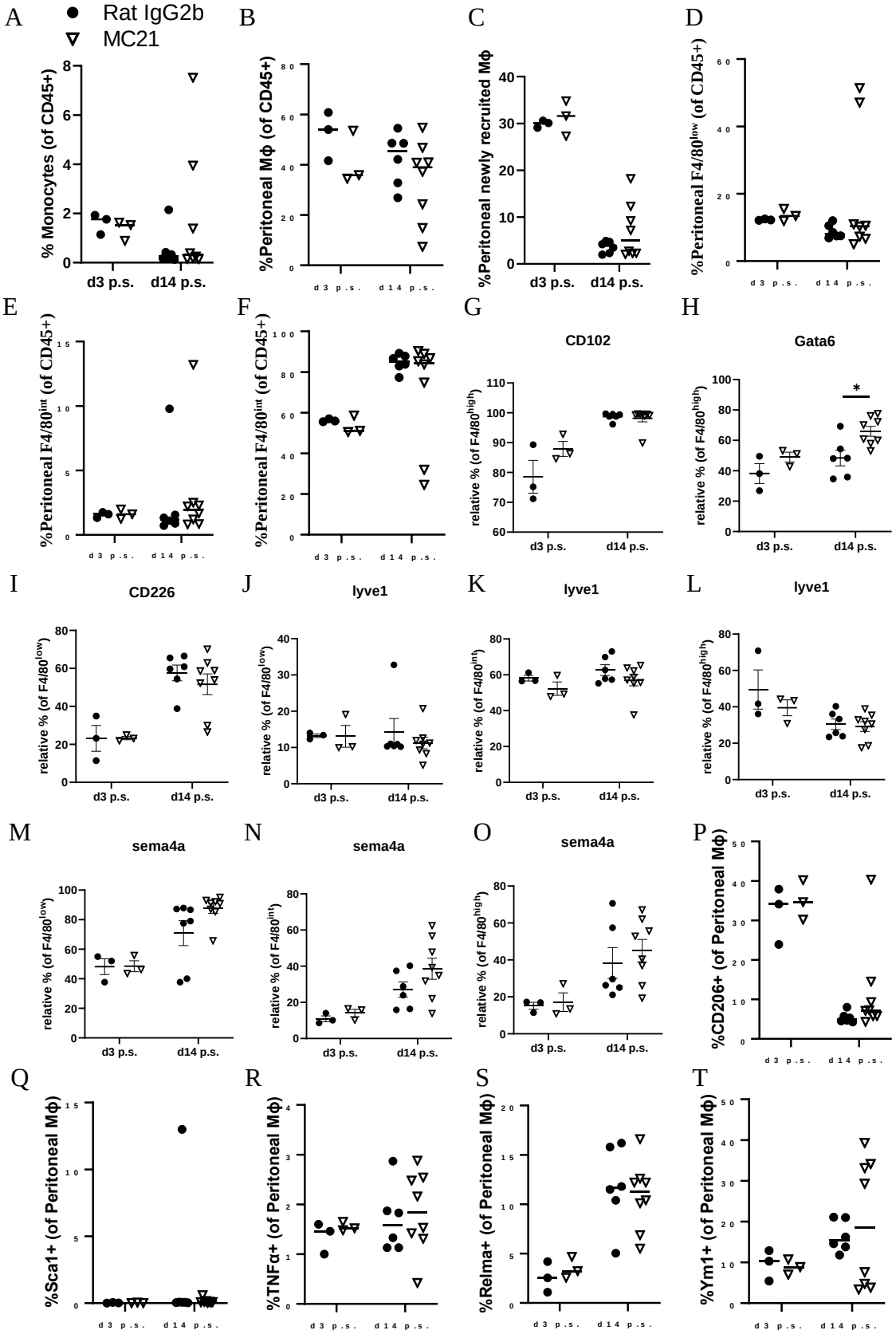

Supplementary Figure 8. Relative percentage of monocytes and different markers of peritoneal macrophages of Rat IgG2b isotype control and anti-CCR2 (clone MC21) treated mice after surgery.

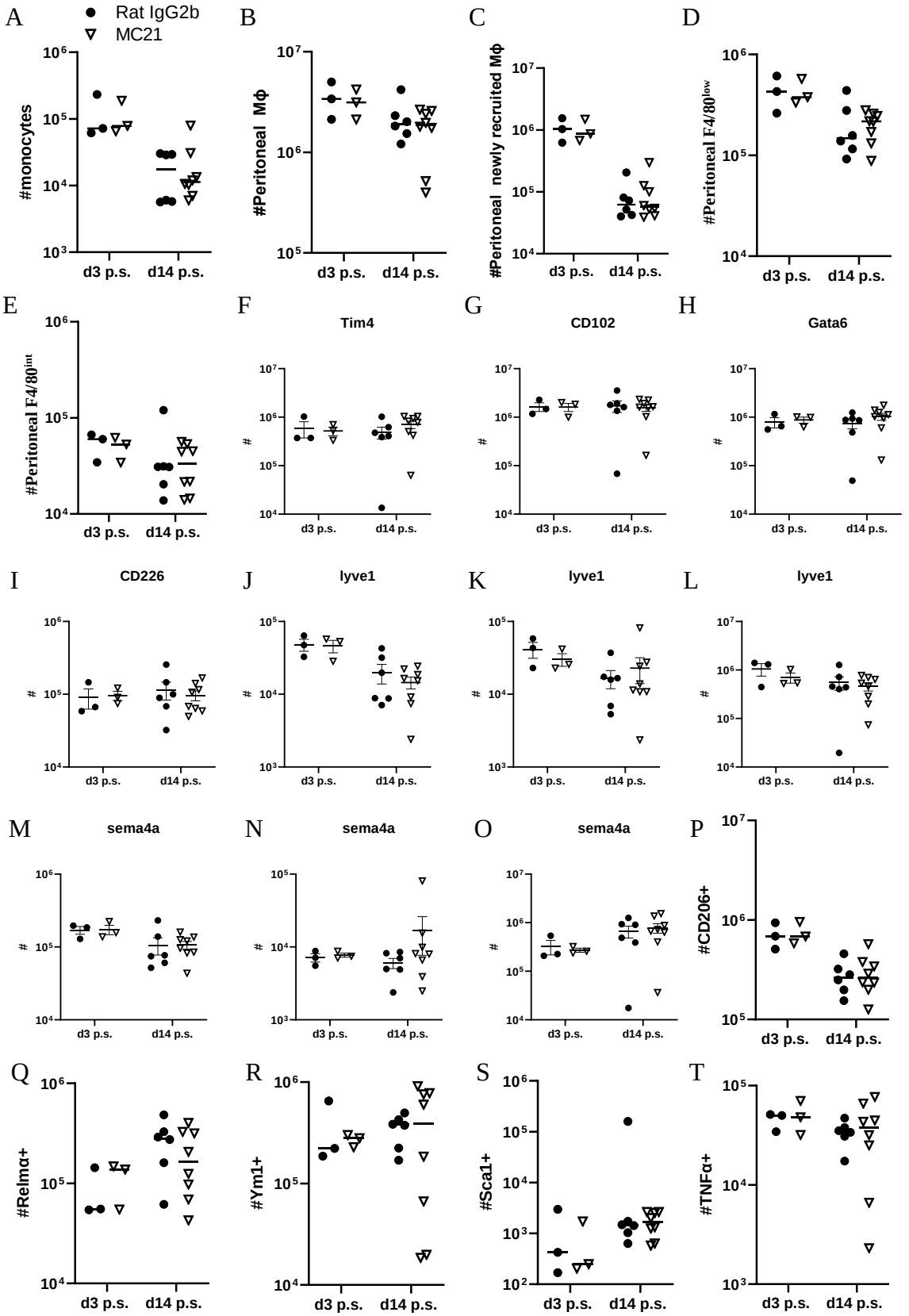

Supplementary Figure 9. Total cell number of monocytes and different markers of peritoneal macrophages of Rat IgG2b isotype control and anti-CCR2 (clone MC21) antibody treated mice after surgery.

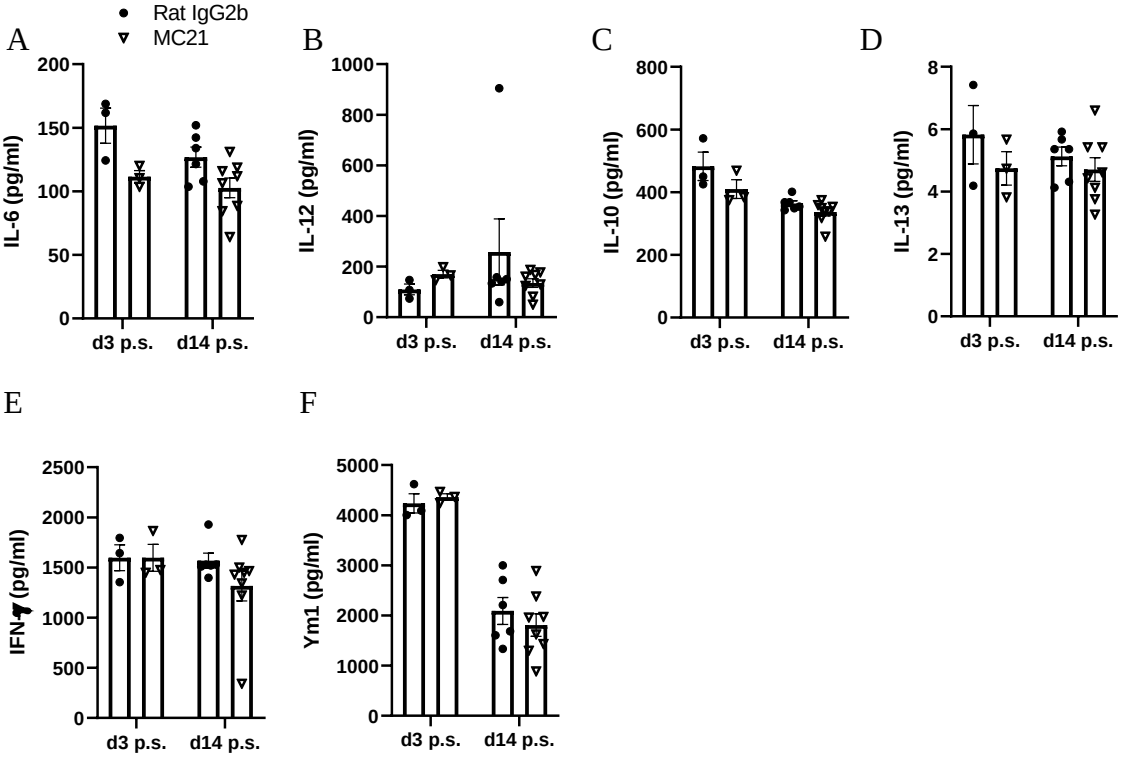

Supplementary Figure 10. Cytokine analysis in the peritoneal lavage of Rat IgG2b isotype control and anti-CCR2 (clone MC21) antibody treated mice after surgery.

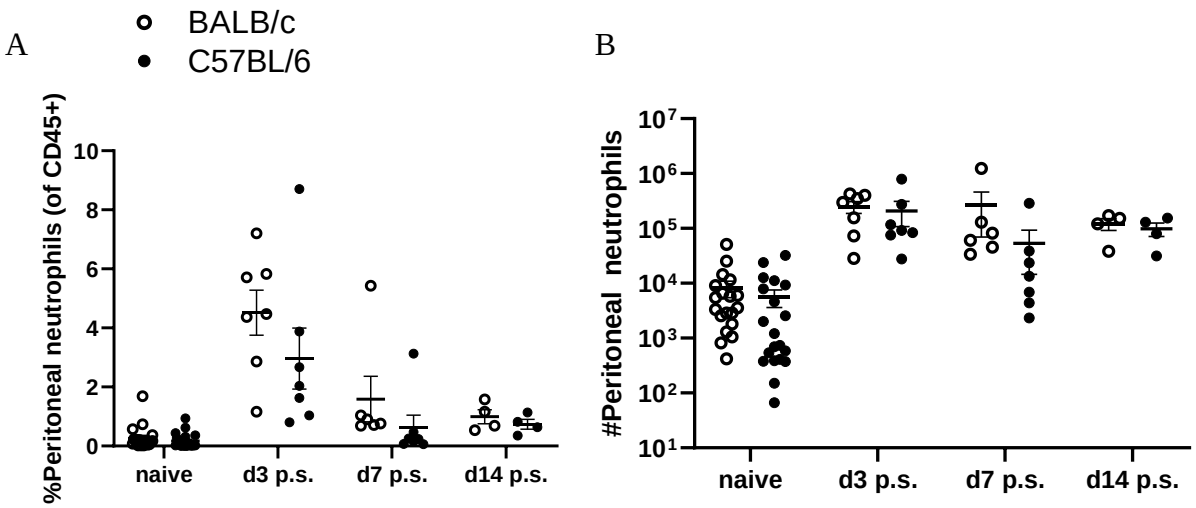

Supplementary Figure 11. The relative percentage and total cell number of neutrophils in the peritoneal cavity of BALB/c and C57BL/6 mice prior and after surgery.